

Title

Role of Triose Phosphate Utilization in photosynthetic response of rice to variable carbon dioxide levels and plant source-sink relations

Running Title

Role of TPU in photosynthesis under source-sink imbalance

Authors

Denis Fabre^{1,2}, Xinyou Yin³, Michael Dingkuhn^{1,2}, Anne Clément-Vidal^{1,2}, Sandrine Roques^{1,2}, Lauriane Rouan^{1,2}, Armelle Soutiras^{1,2}, Delphine Luquet^{1,2}

Contact information

1: CIRAD, UMR AGAP, F-34398 Montpellier, France.

2: Univ Montpellier, CIRAD, INRA, Montpellier SupAgro, Montpellier, France

3: Centre for Crop Systems Analysis, Department of Plant Sciences, Wageningen University & Research, Wageningen, Netherlands

Email address of each authors:

denis.fabre@cirad.fr

xinyou.yin@wur.nl

michael.dingkuhn@cirad.fr

anne.clement-vidal@cirad.fr

sandrine.roques@cirad.fr

lauriane.rouan@cirad.fr

armelle.soutiras@cirad.fr

delphine.luquet@cirad.fr

Corresponding author

Denis Fabre

CIRAD, UMR AGAP, F-34398 Montpellier, France

denis.fabre@cirad.fr

Phone: +33 4 67 61 71 40

Number of tables: 2

Number of figures: 5

Word count: 6270

Number of supplementary data: 5 (4 tables, 1 figure)

Highlight

This study provide new insights in the effect of C source-sink relationships on rice photosynthesis. TPU should be considered in photosynthesis studies under severe source-sink imbalance at elevated CO₂.

Abstract

This study aimed to understand the physiological bases of rice photosynthesis response to C source-sink imbalances, with focus on dynamics of the photosynthetic parameter TPU (Triose Phosphate Utilization). A dedicated experiment was replicated twice on IR64 indica rice cultivar in controlled environments. Plants were grown under the current ambient CO₂ concentration until heading, thereafter, two CO₂ treatments (400 and 800 $\mu\text{mol mol}^{-1}$) were compared in the presence and absence of a panicle pruning treatment modifying the C sink. At two weeks after heading, photosynthetic parameters derived from CO₂ response curves, and nonstructural carbohydrate content of flag leaf and internodes were measured 3-4 times of day. Spikelet number per panicle and flag leaf area on the main culm were recorded. Net C assimilation and TPU decreased progressively after midday in panicle-pruned plants, especially under 800 $\mu\text{mol mol}^{-1}$. This TPU reduction was explained by sucrose accumulation in the flag leaf resulting from the sink limitation. It is suggested that TPU is involved in rice photosynthesis regulation under elevated CO₂ conditions, and that sink limitation effects should be considered in crop models.

Keyword index

Rice; CO₂ enrichment; triose phosphate utilization; source-sink; photosynthesis; sink feedback; sucrose; climate change.

1 **Introduction**

2 Increasing world population and negative effects of global climate change on agricultural
3 production require increased and more climate-resilient crop yields (Ainsworth, 2008; Ort et
4 al., 2015; von Caemmerer et al., 2012). Rice (*Oryza sativa* L.) is the staple food for almost half
5 of the population on Earth (GRiSP, 2013). To meet rice demand in 2050, its production has to
6 increase by 2.4% annually until 2050 (Mohanty et al., 2013; Ray et al., 2013). This must be
7 achieved in the context of climate change that is expected to have mostly negative effects on
8 crop yields (Porter et al., 2014). But air CO₂ elevation (e-CO₂), expected to reach 600 to 700
9 $\mu\text{mol mol}^{-1}$ in 2050 (IPCC 2016), will affect C₃ crops like rice positively if efficiently used by
10 photosynthesis. To achieve the production goal, leaf photosynthesis is a key leverage for
11 improving crops (Evans, 2013; Lawson et al., 2012; Long et al., 2015; Ort et al., 2015),
12 including rice (Makino, 2011; Yoshida et al., 2008; Yoshida and Horie, 2009).

13
14 A key requirement for achieving high crop productivity is to optimize carbon source-sink
15 balance in the plants. E-CO₂ can perturb plant carbon (C) source-sink balance as it can increase
16 C source more than the sink (White et al., 2016), leading to leaf carbohydrate accumulation that
17 may down-regulate photosynthesis (Burnett et al., 2016; Paul and Foyer, 2001; Shimono et al.,
18 2010; White et al., 2016). Source-sink interactions have been intensively studied during the last
19 two decades (Chang et al., 2017). Whether and when plant growth and production is limited by
20 C source (chiefly, photosynthesis) or sink (demand for organ growth) is still a key research
21 question for agronomists, plant physiologists, biochemists and crop modelers (Burnett et al.,
22 2016).

23
24 For agronomists, this question is particularly relevant during the grain filling period (Tang et
25 al., 2017; Wei et al., 2018; Yang and Zhang, 2010; Zhang et al., 2017). Some studies used
26 pruning treatments to manipulate the C source (leaf) and/or sink (grains) (Cock and Yoshida,
27 1973; Hasegawa et al., 2013, 2016; Jing et al., 2016; Nakano et al., 1995, 2017; Shimono et al.,
28 2010; Shinano et al., 2006), and some of these were conducted with an e-CO₂ treatment.
29 Conflicting results were reported regarding the response of photosynthesis to e-CO₂ but all
30 studies agreed that plants with larger sink capacity benefitted more from e-CO₂.

31
32 Several physiological studies dealt with the role of non-structural carbohydrate (NSC) in C
33 source–sink relationships under abiotic constraints such as drought (e.g. Dingkuhn et al., 2007).
34 Experimental manipulations of plant C source and/or sink strength demonstrated that

35 photosynthetic rate depends on C sink strength (Ainsworth and Bush, 2011; Lemoine et al.,
36 2013; Osorio et al., 2014). Accumulation of NSC commonly occurs in leaves of plants grown
37 under e-CO₂ but down-regulation of photosynthesis is not always observed (Leakey et al., 2009;
38 Wang et al., 2015), suggesting that feedbacks on photosynthesis are complex. Part of this
39 complexity might be explained by partitioning of leaf NSC between sucrose and starch,
40 controlled by day length (Mengin et al., 2017; Pokhilko and Ebenhoh, 2015; Sharkey, 2015;
41 Sulpice et al., 2014), other environmental variables such as water deficit (Luquet et al., 2008),
42 or time of day (Bläsing et al., 2005; Gibon et al., 2006). Plants lacking in sink capacity show
43 reduced phloem loading. Rice is particularly effective in its capacity to export NSC from source
44 leaves, suggesting that its photosynthetic response to e-CO₂ should be efficient (Makino and
45 Mae, 1999), but little is known on the mechanisms.

46

47 Biochemical studies on C source-sink relationships have focused on two key parameters: the
48 utilisation of triose phosphate produced in the Calvin cycle for sucrose and starch synthesis,
49 and ribulose biphosphate (RuBP) regeneration by inorganic phosphate (Pi) recycling, which is
50 related to sugar turnover (Leegood and Furbank, 1986; Paul and Foyer, 2001; Paul and Pellny,
51 2003; Sharkey, 1985). Analysis of leaf photosynthesis classically considers three limiting steps
52 according to a biochemical photosynthesis model (the FvCB model hereafter) described by
53 Farquhar et al. (1980), later extended by Sharkey (1985), involving the key parameters: i)
54 Rubisco activity (V_{cmax}), ii) photosynthetic electron transport rate (J_{max}) determining the ability
55 to regenerate RuBP substrate for Rubisco, and iii) Triose Phosphate Utilization (TPU) driving
56 the synthesis of sucrose from sugar precursors in the Calvin-Benson cycle. Thereby, TPU acts
57 as a short-term sink that commits carbon to end-products and is closely linked to triose
58 phosphate conversion into sucrose or starch. High sink capacity accelerates the utilization of
59 triose phosphate for sugar synthesis and export *via* phloem. It accelerates Pi recycling and
60 RuBP regeneration in the Calvin cycle (Gibson et al., 2011; Kant et al., 2012; Kaschuk et al.,
61 2009; Paul and Foyer, 2001; Paul and Pellny, 2003). TPU limitation occurs primarily at high
62 CO₂ or sink-limited situations (Leegood and Furbank, 1986; Sharkey, 1985).

63

64 The FvCB model is commonly used as a module in crop models (Wu et al., 2016). Currently,
65 photosynthesis is thought to be limited mainly by either V_{cmax} or J_{max} , whereas TPU has received
66 less attention and is mostly ignored by crop models (Long and Bernacchi, 2003; von
67 Caemmerer, 2000) because its regulation is largely unknown (Yang et al., 2016). However,
68 TPU as a link between sugar production (source) and consumption (sink) may become

69 functionally important for crop models when addressing future climatic scenarios and e-CO₂
70 (Busch and Sage, 2016), particularly in sink-limiting situations (Asseng et al., 2017;
71 Lombardozzi et al., 2017).

72

73 As the relations between source and sink activities at the crop, plant and process levels are
74 complex, and there is a need to integrate the different levels. For this purpose, the present study
75 aims to explore the role of TPU in the regulation of photosynthesis in response to C source-
76 sink relationships. A dedicated experiment was designed to observe photosynthetic parameters,
77 the dynamics of C source-sink ratio at plant or leaf level, and NSC partitioning between soluble
78 sugars and starch. Results are expected to provide insights on whether TPU influences
79 photosynthetic rate in current and future climatic scenarios, and should thus be considered in
80 crop modelling.

81

82 **Material and methods**

83

84 ***Plant material and growth conditions***

85 Seeds of high yielding *indica* rice cultivar from the Philippines, IR64, were germinated on wet
86 filter paper and transplanted to 4L pots filled with EGO 140 substrate (17%N-10%P-14%K, pH
87 = 5). Basal fertilizer was applied using Basacot 6 M (Compo Expert) at 2 g l⁻¹, 11%N-9%P-
88 19%K +2%Mg. A second application was performed (topdressing) just before the heading stage
89 to avoid post-floral nitrogen deficiency. Experiment was undertaken twice in the same growth
90 chambers, in November 2016 (Exp1) and February 2017 (Exp2), using the same environmental
91 conditions.

92

93 For each experiment, 60 plants were grown and divided between two identical growth chambers
94 (microclima MC1750E, Snijders, Netherlands) at CIRAD, Montpellier, France. The two
95 chambers were maintained at 12-h photoperiod, with day/night temperatures of 29/22°C, air
96 humidity of 65/80% and daytime radiation of 1200 μmol photons m⁻² s⁻¹ photosynthetically
97 active radiation (PAR) at plant tops. The 30 pots per chamber were rotated regularly to
98 compensate for heterogeneity. They were arranged at 35-cm plant spacing in a completely
99 randomized design with five replicates (potted plants). Pots were irrigated to maintain soil
100 moisture at field capacity level.

101

102 At heading stage (80 days after transplanting), all panicles of half of the plants in each growth
103 chamber were excised (pruning treatment PR, first experimental factor). Non-PR plants were
104 called controls. The second factor was CO₂ treatment: In chamber 1, CO₂ level was set at 400
105 $\mu\text{mol mol}^{-1}$ during the whole experiment (ambient treatment); in chamber 2, CO₂ level was
106 maintained at 400 $\mu\text{mol mol}^{-1}$ until the onset of heading, then switched to 800 $\mu\text{mol mol}^{-1}$ (e-
107 CO₂ treatment) for 15 days, the main period of grain filling (Cho et al., 1988). At the end of the
108 e-CO₂ period, physiological and biochemical measurements were performed. The combination
109 of PR and CO₂ treatments at grain filling stage was chosen to achieve maximal C source-
110 sink differences and to avoid the appearance of new sinks (panicles) during differential
111 treatments.

112
113 For Exp1 in each growth chamber, photosynthesis, biochemical and biomass measurements
114 (see details below) were carried out at three times of day: morning, midday, and afternoon, at
115 +1h, +6h, and +9h after dawn, respectively, on 5 consecutive days. Measurements were done
116 on a total of 60 plants (2 PR treatments x 3 times of day of sampling x 2 e-CO₂ levels x 5
117 biological replications).

118
119 For Exp2, in each growth chamber and for each treatment, photosynthesis, biochemical and
120 biomass measurements carried out at midday, afternoon and evening; at +6h, +9h and +11h
121 after dawn, respectively. As for Exp1, these were done for 5 consecutive days, resulting in a
122 total of 60 measured plants.

123

124 ***Leaf photosynthesis measurement***

125 Leaf photosynthesis parameters were measured on the flag leaf on the main culm 2 weeks after
126 heading, using two portable photosynthesis systems (GFS-3100, Walz, Germany) identically
127 calibrated and used to measure simultaneously plants at each CO₂ level. The measurements
128 were made *in situ* using saturating PPFD light (1500 $\mu\text{mol m}^{-2} \text{s}^{-1}$ of PAR), controlled leaf
129 temperature at 29°C, relative humidity in the cuvette set at 65%, and constant air flow rate
130 through the cuvette of 800 ml min^{-1} . We used a large exchange area cuvette of 8 cm^2 to limit
131 border effects known to affect photosynthesis measurement at high [CO₂] (Long and Bernacchi,
132 2003). Net photosynthesis CO₂ response curves (A/C_i) were obtained over a range of external
133 CO₂ levels in the following order: 400, 300, 200, 100, 50, 400, 600, 800, 1000, 1200, 1400,
134 1600, 1800 and 2000 $\mu\text{mol mol}^{-1}$. At each step, gas exchange variables were recorded upon

135 reaching steady-state (7-8 min per step, coefficient of variation <1%). In subsequent analysis,
136 net photosynthesis (A), stomatal conductance (g_s) and intercellular CO₂ concentration (C_i) were
137 determined as the value measured at the 400 $\mu\text{mol mol}^{-1}$ CO₂ step of the curve. Chlorophyll
138 fluorescence was measured for each CO₂ step simultaneously using Walz PAM-fluorimeter
139 3055FL, integrated into the photosynthesis equipment. The steady-state fluorescence yield (F_s)
140 was measured after registering the gas-exchange parameters. A saturating light pulse (8000
141 $\mu\text{mol m}^{-2} \text{s}^{-1}$ during 0.8 s) was applied to achieve the light-adapted maximum fluorescence
142 (F_m'). The operating PSII photochemical efficiency (ϕPSII) was determined as $\phi\text{PSII} = (F_m' -$
143 $F_s)/F_m'$.

144

145 To fit the FvCB model of C₃ photosynthesis to experimental data, we used non-linear fitting
146 procedure developed by Sharkey (2016), version 2, using the Rubisco kinetic parameters
147 determined by temperature response functions according to Bernacchi (2002). The three main
148 photosynthesis limitations, maximum carboxylation rate (V_{cmax}), electron transport rate (J_{max}),
149 and triose phosphate utilisation (TPU), were estimated simultaneously, along with mesophyll
150 conductance (g_m), by minimizing the sum of squares of the residuals. Independent
151 measurements of day-time respiration (R_d) were made on some plants using the procedure of
152 Yin et al. (2011), and an average value of R_d was used as a constant in the fitting procedure to
153 avoid over-parameterization. Fluorescence measurements of ϕPSII were used to study the rate-
154 limiting process for each level on the CO₂ curve, particularly to study the transition to TPU
155 limitation as ϕPSII declines at high C_i (Sharkey 2016). To allow treatment comparisons, all
156 parameters were scaled to a constant temperature of 25°C. In total, 120 CO₂ response curves
157 were analyzed.

158

159 ***Sugar content analysis***

160 Immediately after A/C_i curve measurements, the same leaf was sampled to measure non-
161 structural carbohydrate content (NSC: starch, sucrose, glucose, fructose). Segments of the
162 corresponding culm (top internode below the peduncle and bottom-most elongated internode)
163 were also analyzed. Prior to grinding by ball grinder (Mixer mill MM 200, Retsch, Germany),
164 the samples were frozen in liquid nitrogen. Sugars were extracted 3x from 20 mg samples with
165 1 mL of 80% ethanol for 30 min at 75°C, then centrifuged 10 min at 9500 g (Mikro 200, Hettich
166 centrifuge). Soluble sugars (sucrose, glucose, and fructose) were contained in the supernatant
167 and starch in the sediment. Supernatant was filtered in the presence of polyvinyl

168 polypyrrolidone and activated carbon to eliminate pigments and polyphenols. After evaporation
169 of solute with Speedvac (RC 1022 and RCT 90, Jouan SA, Saint Herblain, France), soluble
170 sugars were quantified by high performance ionic chromatography (HPIC, standard Dionex)
171 with pulsed amperometric detection (HPAE-PAD). The sediment was solubilized with 0.02
172 N NaOH at 90°C for 1.5 h then hydrolyzed with α -amylglucosidase at 50°C, pH 4.2 for 1.5 h.
173 Starch was quantified as described in Boehringer (Pomeranz and Meloan, 1994) with 5 μ L of
174 hexokinase (glucose-6-phosphate dehydrogenase), followed by photometry of NADPH at 340
175 nm (spectrophotometer UV/VIS V-530, Jasco Corporation, Tokyo, Japan).

176

177 ***Leaf Nitrogen Content and Mass per Area***

178 On each plant, segments of the leaf used for measuring CO₂ curve was used for determining
179 the nitrogen content in % dw (Nm; mg N g⁻¹ dw of leaf blade) and specific leaf area (SLA; cm²
180 g⁻¹). Nitrogen content per leaf area (Na; g N m⁻²) was obtained as Nm divided by SLA. The
181 area of each sample was measured with a leaf area meter (Li-3100 Li-Cor) then oven-dried until
182 constant weight (48 h at 70°C). Total nitrogen (N) was analyzed based by Dumas combustion
183 method using a LECO TruMac Nitrogen analyzer, and potassium content (K) was measured in
184 addition in Exp2 using an ICP-OES spectrometer 700 Series (Agilent Technologies). A relative
185 indicator of chlorophyll content, SPAD, was also measured on the same leaf using a SPAD-
186 502 (Minolta, Ltd., Japan).

187

188 ***Plant growth and biomass measurements***

189 After sampling for biochemical analyses, all the aerial parts of plants were collected. Leaf blade,
190 sheath, culm and panicle dw per plant (DM) were measured after drying samples at 70°C during
191 48 h (adding *a posteriori* the DM of organ segments sampled previously). Tillers and panicles
192 were counted and total plant green leaf area measured, using a leaf area meter (Li-3100 Li-Cor,
193 Lincoln, NE, USA). A proxy for the source-sink ratio was estimated at the time of
194 photosynthesis measurements as the main-culm flag leaf area to fertile spikelet number ratio.

195

196 ***Statistical analysis***

197 A three-way analysis of variance (ANOVA) of pruning treatment (PR), CO₂, sampling time
198 and interaction effects on each measured parameter was performed for each experiment
199 combined using the PROC MIXED method of the SAS package (SAS Institute Inc., NC, USA,
200 version 9.04). A multiple comparison of means and Tukey's test ($\alpha=0,05$) was then performed.

201
202 Carbohydrate variables were log-transformed to stabilize variance. An analysis of covariance
203 was performed to study the relationship between TPU, sugar contents, CO₂ and pruning
204 treatments, using the PROC GLIMMIX method of the SAS package. Blocking effects (time of
205 the day) were considered as random effects (Piepho et al., 2003). No experiment effect was
206 observed on parameters measured at the same time in both experiments (illustrated by box plots
207 in Fig. S1 for *A*, TPU and flag leaf sucrose content only).

208

209 **Results**

210

211 *Photosynthetic parameter responses to C source-sink imbalance*

212 Under ambient [CO₂], leaf photosynthesis (*A*) was significantly reduced by PR treatment
213 (P<0.001, Table S1), mainly in the afternoon during which *A* declined for all treatments. This
214 was supported by a significant interaction observed between pruning treatment and time of day
215 of measurement (P<0.001, Table S1). This result was amplified under elevated [CO₂], with a
216 reduction of *A* by 50% in the evening for PR compared to control plants (Fig. 1A).

217

218 No significant effects of the experimental factors were observed on leaf chlorophyll content
219 (SPAD). Stomatal conductance (*g_s*) decreased along the day at both CO₂ concentrations, with
220 significant effects of time of day (P<0.001, Table S1). *g_s* was significantly decreased by PR
221 treatment (P<0.001) which interacted with [CO₂] (P<0.05) without any significant variation of
222 intercellular CO₂ concentration (*C_i*) (Table 1). Decrease of *g_s* was significant only in the
223 afternoon under ambient [CO₂] but already from midday onwards under elevated [CO₂].

224

225 Before estimating *g_m* and other derived parameters from measured *A/C_i* curves, we assessed the
226 shape of *A/C_i* response curves (replicate means) for each treatment along the day (Fig. 2A).
227 Within high *C_i* levels, *A* responded little to a change in *C_i*. It even declined with increasing *C_i*
228 for the PR-treated plants (Fig. 2A), suggesting an inhibition of *A* by TPU limitation. It is
229 difficult to rely on only *A/C_i* curves to determine the transition from RuBP-regeneration
230 limitation to TPU limitation since they usually occur together under high [CO₂] (Bernacchi et
231 al., 2013; Long and Bernacchi, 2003). We used chlorophyll fluorescence-based data on the
232 operating efficiency of PSII electron flow (ϕ PSII) measured concomitantly with *A* to detect the
233 *C_i* above which TPU limited *A*. When this is the case, ϕ PSII declines (Sharkey, 2016). The
234 decline of ϕ PSII was observed above a *C_i* of 825 μ mol mol⁻¹ in the evening, in plants exposed

235 to ambient $[\text{CO}_2]$ and pruning treatment (Fig. 2B, left). It occurred at C_i above 742 and 363
236 $\mu\text{mol mol}^{-1}$ under elevated CO_2 condition in the afternoon and in the evening, respectively (Fig.
237 2B, right). As these C_i thresholds were mostly higher than the C_i at A measurement (Fig. 2B),
238 TPU did not limit A under the experimental conditions. However, under the most severe sink
239 limitation (PR, $800 \mu\text{mol mol}^{-1} [\text{CO}_2]$, evening) TPU was close to limiting levels.

240

241 We applied the procedure of Sharkey (2016) to fit each A/C_i curve to derive estimates of g_m and
242 biochemical photosynthetic parameters. All values of g_m were high, $> 10 \mu\text{mol m}^{-2} \text{s}^{-1} \text{Pa}^{-1}$
243 (Table 1), values known not to limit photosynthesis. Therefore, our estimates of g_m did not
244 explain differences in A among treatments or times of day.

245

246 A significant decrease was observed for V_{cmax} in response to PR treatment (for both
247 experiments: $P < 0.001$, Table S1). However, this reduction depended on CO_2 treatment
248 (interaction PR \times CO_2 at $P < 0.05$, Table S1) and was significant only in the afternoon and
249 evening under elevated CO_2 (Table 1). Mean reduction in PR was 29% compared to control in
250 the afternoon under elevated CO_2 (Fig. 1C). Regarding J_{max} , a significant effect of PR treatment
251 was observed ($P < 0.001$, Table S1), despite no significant numerical decrease of J_{max} in PR
252 treatment compared to control as shown in Table 1 and Fig. 1D. A time-of-day effect was also
253 observed ($P < 0.05$).

254

255 Although A/C_i curves for control plants grown at $400 \mu\text{mol mol}^{-1} [\text{CO}_2]$ did not show TPU
256 limitation (Fig. 2), TPU was significantly reduced by PR treatment ($P < 0.001$, Table S1). A
257 decline of TPU after noon was observed in both $[\text{CO}_2]$ treatments (Fig. 1B), resulting in a highly
258 significant time-of-day effect ($P < 0.001$). This decrease was particularly strong under e- CO_2
259 when combined with PR treatment, which led to significant interaction effects (PR \times CO_2 ,
260 $P < 0.05$). In this latter situation, significant differences between control and PR plants were
261 observed in the afternoon. The decrease of TPU caused by PR in the evening was 40% under
262 elevated $[\text{CO}_2]$ and 13% under ambient $[\text{CO}_2]$ (Fig. 1B).

263

264 *Nonstructural carbohydrate response to C source-sink imbalance*

265 Leaf sucrose concentration in PR plants was significantly higher than in control plants in the
266 afternoon ($P < 0.001$ for both PR and time-of-day effects, Table S2). No interaction effects
267 between these factors were observed. The $[\text{CO}_2]$ effect on leaf sucrose was smaller ($P < 0.05$).
268 Hexose concentration in the flag leaf was not affected by any of the experimental factors.

269

270 PR reduced sucrose concentration in the basal internode on the main culm ($P < 0.001$, Tables 2
271 and S2), without significant variations along the day. Similar results were observed for hexose
272 concentration in the lower internode, but at about 35-fold lower concentrations than sucrose
273 (Table 2). As soluble sugar content (hexose and sucrose) was similar in basal and upper
274 internodes, results are presented only for basal internodes.

275

276 PR increased starch concentration in both top and bottom internodes on the main culm
277 ($P < 0.001$; Tables 2 and S2), whereby no interaction between CO_2 and PR treatments was
278 observed. No time-of-day effect was observed for starch concentration in internodes.

279

280 No PR and CO_2 effects were observed on leaf starch concentration, but there was a significant
281 time-of-day effect ($P < 0.001$, Tables 2 and S2), causing a continuous increase of leaf starch
282 concentration along the day (Table 2).

283

284 ***Plant growth response to C source-sink imbalance***

285 PR significantly increased culm dry matter (by 50-60%, $P < 0.001$, Table S3 and Table S4) and
286 sheath dry matter (by 12-20%, $P < 0.001$). No $[\text{CO}_2]$ effect and no interaction between factors
287 were observed (Table S3). Panicle dry weight sampled two weeks after heading in the control
288 plants was 280% higher under elevated $[\text{CO}_2]$ compared to ambient $[\text{CO}_2]$ ($P < 0.001$, Table S3
289 and Table S4), suggesting a strong stimulation of CO_2 enrichment on grain filling. By contrast,
290 none of the factors affected plant total leaf dry matter, tiller number, panicle number and the
291 SLA of the flag leaves used for photosynthesis measurement (Table S3). The same was true for
292 nitrogen and potassium contents of the flag leaf, except for a significant reduction ($P < 0.05$) of
293 nitrogen content under elevated $[\text{CO}_2]$, particularly on control plants (Table S3 and S4). Dry
294 matter of plant roots was also measured at the end of the experiments. No significant effect of
295 experimental factors were observed (data not presented).

296

297 ***Correlations between photosynthetic and biochemical parameters***

298 A positive linear correlation was observed between A and TPU ($R^2 = 0.64$, $P < 0.001$) across all
299 combinations of $[\text{CO}_2]$ and pruning treatments, and across all times of day (Fig. 3). The
300 strongest treatment-specific correlation was observed when PR treatment was combined with
301 high $[\text{CO}_2]$, i.e. for the treatment combination causing the highest C source-sink ratio ($R^2 = 0.72$,

302 $P < 0.001$). The corresponding correlation between A and V_{cmax} was also significant but weaker
303 ($R^2 = 0.60$; data not presented).

304

305 Analysis of covariance was performed to study the relationship between nonstructural
306 carbohydrate and TPU variations. Flag leaf sucrose concentration was by far the most predictive
307 factor of TPU variation ($P < 0.001$) (Table S5). This was supported by the negative, linear
308 correlations ($R^2 = 0.66$ for controls, $R^2 = 0.40$ for PR) observed between flag leaf sucrose
309 concentration and TPU (Fig. 4). The two linear correlations showed a similar slope (-5.4 for
310 control and -6.1 for pruned) but with lower TPU value at the intercepts in the case of pruned
311 plants. An effect of starch concentration in the lower internodes was also observed ($P = 0.01$)
312 but it was smaller than that of leaf sucrose.

313

314 Finally, a negative correlation was found between TPU and plant C source-sink ratio measured
315 two weeks after heading (R^2 of 0.45, $P < 0.01$; Fig. 5), defined as the ratio of flag leaf area over
316 fertile spikelet number of the corresponding panicle (measured only for Exp2).

317

318 **Discussion**

319 The physiology and biochemistry of leaf photosynthesis of major crops such as rice are well
320 studied. So are the relations between sources, sinks and the formation of grain yield at the plant
321 or crop scale. These processes are necessarily inter-dependent but little is known on the
322 feedbacks causing interaction. We hypothesized that (1) source-sink imbalances are locally
323 expressed as variations of TPU in the leaf, and (2) TPU would limit photosynthetic rate when
324 C_i exceeds a critical level. To test the hypothesis, we manipulated the source with CO_2
325 enrichment and the sink with panicle pruning. The results confirmed hypothesis (1). However,
326 in our experiments C_i did not exceed critical levels causing TPU limitation for A (Hyp.2),
327 although it came close to that level in the afternoon under combined pruning and e- CO_2 . The
328 strong reductions of A , accompanied by local accumulation of assimilates, confirmed the
329 presence of feedback inhibition of photosynthesis under sink limitation.

330

331 ***Photosynthesis down-regulation under C sink limitation***

332 Elevated $[\text{CO}_2]$ enhances plant C source capacity in C_3 plants and potentially, if plant sinks are
333 insufficiently plastic, the C source-sink ratio. Our study showed that photosynthesis decreased
334 along the day. The extent of the decrease depended on C sink limitation induced by sink pruning
335 and/or source stimulation with CO_2 . Declining photosynthesis along the day was previously

336 reported under non-modified C source-sink balance (Ishihara and Saitoh, 1987; Koyama and
337 Takemoto, 2014; Yang et al., 2008). Our observations on control plants under ambient [CO₂]
338 confirmed this trend, whereby enhanced source and pruned sinks further amplified it.
339 Reductions in *A* attained 50% for both factors combined at the end of the day despite constant
340 light resources. Sink limitation effects of this magnitude have not been noticed for rice
341 previously. A similar effect, however, has been reported for wheat (King et al., 1967) after
342 removing ears under ambient [CO₂].

343

344 In the present study, CO₂ enrichment was applied during two weeks following heading. A small
345 but significant reduction of N content per leaf area was observed under high [CO₂], particularly
346 in control plants. As indicated by leaf N concentration per unit dry mass, which was 36 mg g⁻¹
347 for the elevated CO₂ treatment, N was above the empirical observation to affect growth,
348 reported to be 28 mg g⁻¹ (Seneweera et al., 2005: study made at 700 μmol mol⁻¹ CO₂). Leaf N
349 concentration can decrease under CO₂ enrichment due to dilution, causing reduced
350 photosynthesis (Ainsworth and Long, 2005; Leakey et al., 2009; Nakano et al., 1995; Yin
351 2013). This was avoided in this study by limiting CO₂ treatment to two weeks, at a stage when
352 leaves were not expanding anymore. It was also reported that under elevated CO₂ and sink
353 limitation, a high leaf N content could alleviate a photosynthetic down-regulation during the
354 day (Makino et al., 1997; Seneweera et al., 2002). In our experiments, however, a diurnal
355 decline of photosynthesis happened in all treatments despite ample N resources.

356

357 We also investigated leaf potassium concentration in Exp2 because K deficiency potentially
358 affects photosynthesis through stomatal responses *via* osmoregulation in guard cells (Jin et al.,
359 2011; Wang et al., 2013; Weng et al., 2007), and also assimilate transport in phloem
360 (Gerardeaux et al., 2010). No potassium deficiency was observed that could explain the
361 observed variations in photosynthesis.

362

363 A reduction of stomatal conductance was observed under sink pruning treatment, as reported
364 for many plants, e.g., citrus (Nebauer et al., 2011; Urban, 2004) and coffee (DaMatta et al.,
365 2008). Compared to control plants, panicle-pruned plants showed a smaller increase of
366 photosynthetic rate in response to e-CO₂, whereby pruning always reduced stomatal
367 conductance. However, there was no significant difference in *C_i* between control and pruned
368 plants when measured at a given atmospheric [CO₂]. Pruning thus decreased *A* at an unchanged
369 *C_i* level, indicating that the photosynthetic capacity of the leaf was affected. Shimono et al.

370 (2010) also reported that rice plants with pruned panicles under ambient and elevated CO₂ had
371 unaltered C_i levels.

372

373 No CO₂ effect was observed on stomatal conductance, in contrast to reports by Ainsworth
374 (2008) and Yoshimoto et al. (2005). In our study, a supplemental dose of N fertilizer was
375 applied just before heading stage. This might have maintained high stomatal conductance as
376 previously shown in rice (Shimoda, 2012; Shimoda and Maruyama, 2014). Similar to another
377 study evaluating short-term CO₂ enrichment effects on mesophyll conductance (Tazoe et al.,
378 2009), no PR and CO₂ effect was observed on mesophyll conductance g_m, a parameter known
379 to be sensitive to environment and estimation method (Flexas et al., 2008; Pons et al., 2009;
380 Singaas et al., 2004; Sun et al., 2014). In our experimental conditions involving a 14-day CO₂
381 enrichment, g_m was very high and thus did not limit photosynthesis. Rice generally has high g_m
382 as compared with other species (van der Putten et al., 2018), probably because rice leaves have
383 high chloroplasts coverage on the mesophyll cell periphery (Busch et al., 2013). Therefore, g_m
384 was not responsible for the decline in *A* observed under sink limitation. In addition, no
385 difference was observed for SLA, a morphological trait that can affect genotypic photosynthetic
386 capacity (Dingkuhn et al., 1998).

387

388 The down-regulation of photosynthesis observed under elevated CO₂ in the afternoon under C
389 source-sink imbalance is a phenomenon that escapes observation if photosynthesis time courses
390 are studied day-to-day and not within the day. This phenomenon is not captured in
391 measurements at daily intervals (e.g., Makino and Mae, 1999), commonly done in the morning
392 or at noon (Pérez-Harguindeguy et al., 2013). Our results suggest that it is crucial to capture
393 diurnal changes of photosynthesis when studying source-sink effects on photosynthetic rate, or
394 when estimating cumulative photosynthesis for a day.

395

396 ***TPU effect on photosynthesis under sink limitation***

397 Generally, there are transitions from one limiting factor to another, although they may be
398 masked by a concomitant decline of several factors through feedbacks. Along *A/C_i* curves, *A* is
399 limited by Rubisco activity (characterized by *V_{cmax}*) at low C_i, by RuBP regeneration
400 (characterized by *J_{max}*) at higher C_i, and potentially by TPU at even higher C_i. A TPU limitation
401 is characterized by a lack of sensitivity of *A* to, or by a slight decline of *A* with, increases of
402 CO₂ partial pressure (Sharkey, 1985). TPU limitation can be further ascertained by a decline of
403 φPSII with increasing C_i (Sharkey, 2016). When TPU limitation occurs, photosynthesis is

404 affected by shortage of Pi (Paul and Foyer, 2001; Sharkey and Vanderveer, 1989) needed for
405 ATP synthesis. In the absence of a strong C sink, TPU can be rate-limited by sucrose synthesis,
406 thereby decreasing Pi recycling rate (Paul and Pellny, 2003). This limited regeneration is
407 reflected in the rate at which the intermediate products of CO₂ fixation (triose-phosphate) are
408 converted to starch and sucrose and accumulated locally.

409
410 The patterns of diurnal decline of TPU generally mirrored those of *A* (Fig. 1), resulting in a
411 highly significant correlation between the two variables (Fig. 3). This correlation in itself,
412 however, is not proof of a rate limitation by TPU. The *A/C_i* curves in Fig. 2A suggest that with
413 increasing sink limitation (combinations of factors e-CO₂, pruning, time of day), *A* tended to
414 plateau, or even decline, at high *C_i* values. Chlorophyll fluorescence-based quantum yield
415 efficiency, measured concurrently with gas exchange under exposure to 14 levels of [CO₂],
416 indicated the critical *C_i* above which TPU limited *A* for each treatment (Fig. 2B). In most of the
417 situations studied, the critical *C_i* incurring TPU limitation was higher than the observed *C_i*. In
418 one particular situation, however (e-CO₂, pruning, evening), the critical *C_i* was 363 μmol mol⁻¹
419 and thus, similar to the observed *C_i* value. Consequently, although TPU decreased most strongly
420 among the biochemical photosynthetic parameters under sink limitation, it probably did not
421 limit *A* except, possibly, for the treatment causing the strongest source-sink imbalance.

422
423 Further studies should determine if TPU can limit *A* in a climate change context with elevated
424 ambient CO₂, and/or under lower temperatures to which TPU is very sensitive (Busch and Sage,
425 2016; Cen and Sage, 2005), and for plants having lesser phenotypic plasticity and assimilate
426 transport capacity than rice. TPU limitations have been reported under low temperature (Sage
427 and Kubien, 2007; Sage and Sharkey, 1987) or high CO₂ environments (Cen and Sage, 2005;
428 Sharkey et al., 1986). In such cases, mutual adjustment of *V_{cmax}* and TPU is observed, as these
429 parameters decrease concurrently and in strict stoichiometry (McClain and Sharkey, 2018).
430 Indeed, we observed a strong decrease of *V_{cmax}* at high [CO₂] in the pruned plants (Fig. 1)
431 concurrently with TPU, suggesting a co-adjustment. Changes in *V_{cmax}* may have contributed to
432 the observed decrease in photosynthesis under e-CO₂ (Makino et al., 2000; Shimono et al.,
433 2010), possibly due to a loss of Rubisco (Long et al., 2004). It was also shown that TPU
434 limitation activates energy-dependent quenching (*q_E*), resulting in a deactivation of Rubisco
435 (Sage et al., 1989; Sharkey et al., 1986). To enable photosynthesis, the carbon reduction cycle
436 needs to regenerate RuBP, consuming ATP and NADPH produced through photosynthetic
437 electron transport in the chloroplast. This process can be evaluated by *J_{max}* parameter (RuBP

438 regeneration) which can also limit photosynthesis. Although we observed a significant decrease
439 in J_{\max} during the day in response to sink pruning, variations were too small to explain the
440 observed variation of A . The two parameters correlating most with A were V_{\max} and TPU,
441 suggesting a tight coordination between TPU and Rubisco capacity.

442

443 Our findings suggest that TPU and A of rice generally decline in the afternoon, and particularly
444 when sink is restricted. This may potentially cause overestimation of whole-day photosynthesis
445 in crop models that do not consider rate limitations to assimilate export from the leaf
446 (Lombardozzi et al., 2017, 2018). TPU is situated at the interface between production and
447 consumption (or removal) of photosynthates. Thus, the mechanisms controlling this parameter
448 can only be understood in a whole-plant context including assimilate transport and partitioning
449 among sinkd (Yang et al., 2016).

450

451 ***Sugar partitioning effect on photosynthesis and TPU regulation***

452 Similar to our results, Morita et al., (2016), Shimono et al. (2010), Thompson et al. (2017) and
453 Zhu et al. (2016) found that leaf sucrose concentration increased more than hexose
454 concentrations under e-CO₂. No increase in starch concentration in the flag leaf was observed
455 under those conditions (Shimono et al., 2010). This can be explained by the large capacity of
456 rice to accumulate carbohydrates in culm. Moreover, leaf starch concentration in the flag leaf
457 (100 to 300 $\mu\text{g cm}^{-2}$) was below empirical critical values (600 $\mu\text{g cm}^{-2}$) reported to affect
458 photosynthesis in rice (Weng and Chen, 1991), suggesting that leaf starch accumulation did not
459 affect A .

460

461 We observed an increase in starch concentration in culm internodes in panicle-pruned plants,
462 probably because internodes acted as alternative sinks for the panicle. Culm sucrose
463 remobilization decreased under pruning and possibly explained the increase in starch. It may
464 have acted as a physiological signal regulating photosynthesis as reported for sugarcane
465 (McCormick et al., 2009; Wang et al., 2018).

466

467 Flag leaf sucrose concentration was identified as the main nonstructural carbohydrate affected
468 by pruning treatment and [CO₂], showing a continuous increase along the day. Photosynthesis
469 is inhibited by leaf carbohydrate accumulation (Goldschmidt and Huber, 1992; Paul and Pellny,
470 2003). In this study, a negative linear relation was observed between TPU and leaf sucrose
471 content. A theory of TPU control by Pi availability, mediated by sugar production, was

472 proposed by Paul and Pellny (2003). According to this theory, TPU can limit photosynthetic
473 rate through a reduced export carbon from the Calvin-Benson cycle, which in turn is related to
474 the rate at which sugar phosphates are dephosphorylated and end-products are produced. Thus,
475 the production and export of sucrose is essential for sustaining photosynthesis. We suggest that
476 in our study, leaf sucrose was exported to plant sinks such as the panicle in control plants,
477 preventing excessive build-up in the leaf. For panicle-pruned plants, sucrose could not be
478 exported sufficiently during the afternoon. Some export occurred to the top internode, where
479 starch concentration increased, but sucrose concentration increased in the flag leaf due to the
480 smaller sink (Huber and Huber, 1992; Paul and Foyer, 2001). In this case, Sucrose Phosphate
481 Synthase (SPS) feedback inhibition occurs because of an increase in the phosphorylation state
482 of the enzyme (Huber et al., 1989). It has been shown that SPS is a substrate for SNF-1 related
483 protein kinases, modulating SPS activity when sucrose accumulates (Sugden et al., 1999).
484 Inhibition of sucrose synthesis may reduce export of TP from the chloroplast, causing a drop in
485 Pi in the cytosol, leading to decrease in TPU (Paul and Pellny, 2003).

486
487 While the negative correlation between TPU and flag-leaf sucrose concentration showed a
488 similar slope for the panicle-pruned and control plants, TPU was lower in the pruning treatment
489 at any given sucrose concentration (reduced intercept, Fig. 4). Thus, the TPU vs. [sucrose]
490 relationship was not the same for control and panicle-pruning treatments, and [sucrose] alone
491 could not explain the TPU decline under C source-sink imbalance. Possibly, additional
492 feedbacks on TPU occurred, e.g. via phloem sucrose concentration. Sucrose concentration in
493 the leaf phloem depends on the rate of sucrose loading at the source and unloading at the sink
494 end (Chiou and Bush, 1998; Li et al., 2003). Panicle pruning probably led to high sucrose
495 concentrations in the leaf phloem as sucrose transport is mainly operated by phloem in rice
496 (Regmi et al., 2016). Photo-assimilates would build up in the mesophyll (Chiou and Bush,
497 1998) and decrease TPU as previously described.

498
499 The ratio of flag-leaf area over the fertile spikelet number of the corresponding panicle provides
500 a rough proxy for local C source-sink ratio during grain filling. It correlated negatively with
501 TPU (Fig. 5), suggesting that morphology-based phenotypic plasticity causing variation in C
502 source-sink ratio can affect TPU. A recent study also reported the effect of sink strength on
503 sucrose partitioning that may be used to increase grain yield in rice (Morey et al., 2018). More
504 research is needed to understand how whole-plant source-sink interactions affect crops' ability
505 to utilize rising CO₂ levels.

506

507 This study provided new insights into the effect of C source-sink relationships on rice
508 photosynthesis and in particular, its parameter TPU. A significant down-regulation of
509 photosynthesis (up to 50%) was demonstrated during the 2nd half of the day in response to sink
510 limitation. TPU strongly decreased along with *A* and it was negatively correlated with flag-leaf
511 sucrose concentration, suggesting sugar feedback inhibition of *A*. It is suggested that
512 photosynthesis measurements performed in the morning, as commonly practiced, may not
513 reliably represent the plant's diurnal photosynthetic performance, particularly under CO₂
514 enrichment or sink limitation.

515 Although TPU decline mirrored the decline of *A* under sink limitation, its rate-limiting effect
516 on *A* could not be confirmed, except possibly at the end of the day for the combination of e-
517 CO₂ and panicle pruning. Only under these specific conditions, the observed *C*_i was similar to
518 the critical *C*_i above which quantum yield efficiency decreased. TPU may thus play an
519 important role in photosynthesis regulation only under extreme source-sink imbalance that may
520 occur in plants that poorly adjust sinks and assimilate transport to increased assimilation
521 potential.

522 Based on these results, it will be interesting to explore the photosynthetic responses of
523 genotypes differing in source-sink ratio and the adaptive plasticity of sinks in CO₂-enriched
524 environments.

525

526 **Acknowledgments**

527 This work was financially supported by CIRAD, French Agricultural Research Centre for
528 International Development; <http://www.cirad.fr>). We thank Audrey Dardou, Paul Pruvost,
529 Christian Chaine, Remy Michel for their valuable assistance in technical support, and the
530 biochemical phenotyping platform of the AGAP research unit at CIRAD.

531

532 **Supplementary data**

533 **Fig. S1:** Boxplot on various parameters for the two experiments

534 **Table S1:** Summary of 3-way analysis of variance of physiological flag leaf variables

535 **Table S2:** Summary of 3-way analysis of variance of non-structural carbohydrate
536 concentrations

537 **Table S3:** Summary of 3-way analysis of variance of plant biomass and morphological
538 variables

539 **Table S4:** Plant growth characteristics

540 **Table S5:** Type III test of fixed effects for co-variance analysis for TPU with carbohydrates
541 and treatment

542

543 **References**

544 **Ainsworth EA.** 2008. Rice production in a changing climate: a meta-analysis of responses to
545 elevated carbon dioxide and elevated ozone concentration. *Global Change Biology* **14**, 1642–
546 1650.

547 **Ainsworth EA, Bush DR.** 2011. Carbohydrate Export from the Leaf: A Highly Regulated
548 Process and Target to Enhance Photosynthesis and Productivity. *PLANT PHYSIOLOGY*
549 **155**, 64–69.

550 **Ainsworth EA, Long SP.** 2005. What have we learned from 15 years of free-air CO₂
551 enrichment (FACE)? A meta-analytic review of the responses of photosynthesis, canopy
552 properties and plant production to rising CO₂. *New Phytologist* **165**, 351–372.

553 **Asseng S, Kassie BT, Labra MH, Amador C, Calderini DF.** 2017. Simulating the impact
554 of source-sink manipulations in wheat. *Field Crops Research* **202**, 47–56.

555 **Bernacchi CJ.** 2002. Temperature Response of Mesophyll Conductance. Implications for the
556 Determination of Rubisco Enzyme Kinetics and for Limitations to Photosynthesis in Vivo.
557 *PLANT PHYSIOLOGY* **130**, 1992–1998.

558 **Bernacchi CJ, Bagley JE, Serbin SP, Ruiz-Vera UM, Rosenthal DM, Vanloocke A.** 2013.
559 Modelling C₃ photosynthesis from the chloroplast to the ecosystem. *Plant, Cell &*
560 *Environment* **36**, 1641–1657.

561 **Bläsing OE, Gibon Y, Günther M, Höhne M, Morcuende R, Osuna D, Thimm O, Usadel**
562 **B, Scheible W-R, Stitt M.** 2005. Sugars and Circadian Regulation Make Major Contributions
563 to the Global Regulation of Diurnal Gene Expression in Arabidopsis *The Plant Cell* **17**, 3257–
564 3281.

565 **Burnett AC, Rogers A, Rees M, Osborne CP.** 2016. Carbon source-sink limitations differ
566 between two species with contrasting growth strategies: Source-sink limitations vary with
567 growth strategy. *Plant, Cell & Environment* **39**, 2460–2472.

568 **Busch FA, Sage RF.** 2016. The sensitivity of photosynthesis to O₂ and CO₂ concentration
569 identifies strong Rubisco control above the thermal optimum. *New Phytologist*.

570 **Busch FA, Sage TL, Cousins AB, Sage RF.** 2013. C₃ plants enhance rates of photosynthesis
571 by reassimilating photorespired and respired CO₂. *Plant, Cell & Environment* **36**, 200–212.

- 572 **von Caemmerer S.** 2000. *Biochemical Models of Leaf Photosynthesis*.
- 573 **von Caemmerer S, Quick WP, Furbank RT.** 2012. The Development of C4 Rice: Current
574 Progress and Future Challenges. *Science* **336**, 1671–1672.
- 575 **Cen Y-P, Sage RF.** 2005. The Regulation of Rubisco Activity in Response to Variation in
576 Temperature and Atmospheric CO₂ Partial Pressure in Sweet Potato. *Plant Physiology* **139**,
577 979–990.
- 578 **Chang T-G, Zhu X-G, Raines C.** 2017. Source-sink interaction: a century old concept under
579 the light of modern molecular systems biology. *Journal of Experimental Botany* **68**, 4417–
580 4431.
- 581 **Chiou TJ, Bush DR.** 1998. Sucrose is a signal molecule in assimilate partitioning.
582 *Proceedings of the National Academy of Sciences of the United States of America* **95**, 4784–
583 4788.
- 584 **Cho D, Jong S, Son S, Park YK.** 1988. Studies on the duration and rate of grain filling in
585 rice (*Oryza sativa* L.). II. Difference between the parts of a panicle. *Kor J Crop Sci*, 5–11.
- 586 **Cock JH, Yoshida S.** 1973. Changing sink and source relations in rice (*Oryza sativa* L.)
587 using carbon dioxide enrichment in the field. *Soil Science and Plant Nutrition* **19**, 229–234.
- 588 **DaMatta FM, Cunha RL, Antunes WC, Martins SCV, Araujo WL, Fernie AR, Moraes**
589 **GABK.** 2008. In field-grown coffee trees source-sink manipulation alters photosynthetic
590 rates, independently of carbon metabolism, via alterations in stomatal function. *The New*
591 *Phytologist* **178**, 348–357.
- 592 **Dingkuhn M, Jones MP, Johnson DE, Sow A.** 1998. Growth and yield potential of *Oryza*
593 *sativa* and *O. glaberrima* upland rice cultivars and their interspecific progenies. *Field Crops*
594 *Research* **57**, 57–69.
- 595 **Dingkuhn M, Luquet D, Clément-Vidal A, Tambour L, Kim HK, Song YH.** 2007. Is
596 plant growth driven by sink regulation? Implications for crop models, phenotyping
597 approaches and ideotypes. *Frontis* **21**, 155–168.
- 598 **Evans JR.** 2013. Improving Photosynthesis. *PLANT PHYSIOLOGY* **162**, 1780–1793.
- 599 **Farquhar G v, von Caemmerer S von, Berry JA.** 1980. A biochemical model of
600 photosynthetic CO₂ assimilation in leaves of C₃ species. *Planta* **149**, 78–90.
- 601 **Flexas J, Ribas-Carbó M, Diaz-Espejo A, Galmés J, Medrano H.** 2008. Mesophyll
602 conductance to CO₂: current knowledge and future prospects. *Plant, Cell & Environment* **31**,
603 602–621.
- 604 **Gerardeaux E, Jordan-Meille L, Constantin J, Pellerin S, Dingkuhn M.** 2010. Changes in
605 plant morphology and dry matter partitioning caused by potassium deficiency in *Gossypium*

- 606 *hirsutum* (L.). *Environmental and Experimental Botany* **67**, 451–459.
- 607 **Gibon Y, Usadel B, Blaesing OE, Kamlage B, Hoehne M, Trethewey R, Stitt M.** 2006.
- 608 Integration of metabolite with transcript and enzyme activity profiling during diurnal cycles in
- 609 *Arabidopsis* rosettes. *Genome Biology* **7**, R76.
- 610 **Gibson K, Park J-S, Nagai Y, et al.** 2011. Exploiting leaf starch synthesis as a transient sink
- 611 to elevate photosynthesis, plant productivity and yields. *Plant Science* **181**, 275–281.
- 612 **Goldschmidt EE, Huber SC.** 1992. Regulation of Photosynthesis by End-Product
- 613 Accumulation in Leaves of Plants Storing Starch, Sucrose, and Hexose Sugars. *Plant*
- 614 *Physiology* **99**, 1443–1448.
- 615 **Hasegawa T, Sakai H, Tokida T, et al.** 2013. Rice cultivar responses to elevated CO₂ at two
- 616 free-air CO₂ enrichment (FACE) sites in Japan. *Functional Plant Biology* **40**, 148.
- 617 **Hasegawa T, Sakai H, Tokida T, Usui Y, Yoshimoto M, Fukuoka M, Nakamura H,**
- 618 **Shimono H, Okada M.** 2016. Rice Free-Air Carbon Dioxide Enrichment Studies to Improve
- 619 Assessment of Climate Change Effects on Rice Agriculture. *Improving Modeling Tools to*
- 620 *Assess Climate Change Effects on Crop Response* **advancesinagric**, 45–68.
- 621 **Huber SC, Huber JL.** 1992. Role of Sucrose-Phosphate Synthase in Sucrose Metabolism in
- 622 Leaves. *Plant Physiology* **99**, 1275–1278.
- 623 **Huber JL, Huber SC, Nielsen TH.** 1989. Protein phosphorylation as a mechanism for
- 624 regulation of spinach leaf sucrose-phosphate synthase activity. *Archives of Biochemistry and*
- 625 *Biophysics* **270**, 681–690.
- 626 **Ishihara K, Saitoh K.** 1987. Diurnal Courses of Photosynthesis, Transpiration, and Diffusive
- 627 Conductance in the Single-leaf of the Rice Plants Grown in the Paddy Field under Submerged
- 628 Condition. *Japanese Journal of Crop Science* **56**, 8–17.
- 629 **Jin SH, Huang JQ, Li XQ, Zheng BS, Wu JS, Wang ZJ, Liu GH, Chen M.** 2011. Effects
- 630 of potassium supply on limitations of photosynthesis by mesophyll diffusion conductance in
- 631 *Carya cathayensis*. *Tree Physiology* **31**, 1142–1151.
- 632 **Jing L, Wu Y, Zhuang S, Wang Y, Zhu J, Wang Y, Yang L.** 2016. Effects of CO₂
- 633 enrichment and spikelet removal on rice quality under open-air field conditions. *Journal of*
- 634 *Integrative Agriculture* **15**, 2012–2022.
- 635 **Kant S, Seneweera S, Rodin J, Materne M, Burch D, Rothstein SJ, Spangenberg G.**
- 636 2012. Improving yield potential in crops under elevated CO₂: Integrating the photosynthetic
- 637 and nitrogen utilization efficiencies. *Frontiers in Plant Science* **3**.
- 638 **Kaschuk G, Kuyper TW, Leffelaar PA, Hungria M, Giller KE.** 2009. Are the rates of
- 639 photosynthesis stimulated by the carbon sink strength of rhizobial and arbuscular mycorrhizal

- 640 symbioses? *Soil Biology and Biochemistry* **41**, 1233–1244.
- 641 **King RW, Wardlaw IF, Evans LT.** 1967. Effect of assimilate utilization on photosynthetic
642 rate in wheat. *Planta* **77**, 261–276.
- 643 **Koyama K, Takemoto S.** 2014. Morning reduction of photosynthetic capacity before midday
644 depression. *Scientific Reports* **4**.
- 645 **Lawson T, Kramer DM, Raines CA.** 2012. Improving yield by exploiting mechanisms
646 underlying natural variation of photosynthesis. *Current Opinion in Biotechnology* **23**, 215–
647 220.
- 648 **Leakey ADB, Ainsworth EA, Bernacchi CJ, Rogers A, Long SP, Ort DR.** 2009. Elevated
649 CO₂ effects on plant carbon, nitrogen, and water relations: six important lessons from FACE.
650 *Journal of Experimental Botany* **60**, 2859–2876.
- 651 **Leegood RC, Furbank RT.** 1986. Stimulation of photosynthesis by 2% oxygen at low
652 temperatures is restored by phosphate. *Planta* **168**, 84–93.
- 653 **Lemoine R, Camera SL, Atanassova R, et al.** 2013. Source-to-sink transport of sugar and
654 regulation by environmental factors. *Frontiers in Plant Science* **4**.
- 655 **LI C, WEISS D, GOLDSCHMIDT EE.** 2003. Girdling Affects Carbohydrate-related Gene
656 Expression in Leaves, Bark and Roots of Alternate-bearing Citrus Trees. *Annals of Botany*
657 **92**, 137–143.
- 658 **Lombardozzi D, Smith NG, Cheng SJ, Bonan GB, Dukes JS, Fisher R, Sharkey TD,**
659 **Rogers A.** 2017. The impact of including export limitation in photosynthetic models from
660 leaf to global scales. *AGU Fall Meeting Abstracts* **21**.
- 661 **Lombardozzi DL, Smith NG, Cheng SJ, Dukes JS, Sharkey TD, Alistair Rogers, Fisher**
662 **R, Bonan GB.** 2018. Triose phosphate limitation in photosynthesis models reduces leaf
663 photosynthesis and global terrestrial carbon storage. *Environmental Research Letters* **13**,
664 074025.
- 665 **Long SP, Ainsworth EA, Rogers A, Ort DR.** 2004. Rising atmospheric carbon dioxide:
666 plants FACE the Future*. *Annu. Rev. Plant Biol.* **55**, 591–628.
- 667 **Long SP, Bernacchi CJ.** 2003. Gas exchange measurements, what can they tell us about the
668 underlying limitations to photosynthesis? Procedures and sources of error. *Journal of*
669 *Experimental Botany* **54**, 2393–2401.
- 670 **Long SP, Marshall-Colon A, Zhu X-G.** 2015. Meeting the Global Food Demand of the
671 Future by Engineering Crop Photosynthesis and Yield Potential. *Cell* **161**, 56–66.
- 672 **Luquet D, Clément-Vidal A, Fabre D, This D, Sonderegger N, Dingkuhn M.** 2008.
673 *Orchestration of transpiration, growth and carbohydrate dynamics in rice during a dry-down*

- 674 cycle. *Functional Plant Biology* **35**, 689–704.
- 675 **Makino A**. 2011. Photosynthesis, Grain Yield, and Nitrogen Utilization in Rice and Wheat.
676 *Plant Physiology* **155**, 125–129.
- 677 **Makino A, Harada M, Sato T, Nakano H, Mae T**. 1997. Growth and N allocation in rice
678 plants under CO₂ enrichment. *Plant Physiology* **115**, 199–203.
- 679 **Makino A, Mae T**. 1999. Photosynthesis and plant growth at elevated levels of CO₂. *Plant*
680 *and Cell Physiology* **40**, 999–1006.
- 681 **Makino A, Nakano H, Mae T, Shimada T, Yamamoto N**. 2000. Photosynthesis, plant
682 growth and N allocation in transgenic rice plants with decreased Rubisco under CO₂
683 enrichment. *Journal of Experimental Botany* **51**, 383–389.
- 684 **McClain AM, Sharkey TD**. 2018. Triose phosphate utilization and beyond: from
685 photosynthesis to end-product synthesis. *bioRxiv*, 434928.
- 686 **McCormick AJ, Watt DA, Cramer MD**. 2009. Supply and demand: sink regulation of sugar
687 accumulation in sugarcane. *Journal of Experimental Botany* **60**, 357–364.
- 688 **Mengin V, Pyl E-T, Alexandre Moraes T, Sulpice R, Krohn N, Encke B, Stitt M**. 2017.
689 Photosynthate partitioning to starch in *Arabidopsis thaliana* is insensitive to light intensity but
690 sensitive to photoperiod due to a restriction on growth in the light in short photoperiods.
691 *Plant, Cell & Environment* **40**, 2608–2627.
- 692 **Mohanty S, Wassmann R, Nelson A, Moya P, Jagadish SVK**. 2013. Rice and climate
693 change: significance for food security and vulnerability. International Rice Research Institute.
- 694 **Morey SR, Hirose T, Hashida Y, Miyao A, Hirochika H, Ohsugi R, Yamagishi J, Aoki**
695 **N**. 2018. Genetic Evidence for the Role of a Rice Vacuolar Invertase as a Molecular Sink
696 Strength Determinant. *Rice* **11**.
- 697 **Morita R, Inoue K, Ikeda K, Hatanaka T, Misoo S, Fukayama H**. 2016. Starch Content in
698 Leaf Sheath Controlled by CO₂-Responsive CCT Protein is a Potential Determinant of
699 Photosynthetic Capacity in Rice. *Plant and Cell Physiology* **57**, 2334–2341.
- 700 **Nakano H, Makino A, Mae T**. 1995. Effects of panicle removal on the photosynthetic
701 characteristics of the flag leaf of rice plants during the ripening stage. *Plant and cell*
702 *physiology* **36**, 653–659.
- 703 **Nakano H, Yoshinaga S, Takai T, et al**. 2017. Quantitative trait loci for large sink capacity
704 enhance rice grain yield under free-air CO₂ enrichment conditions. *Scientific Reports* **7**.
- 705 **Nebauer SG, Renau-Morata B, Guardiola JL, Molina R-V**. 2011. Photosynthesis down-
706 regulation precedes carbohydrate accumulation under sink limitation in Citrus. *Tree*
707 *Physiology* **31**, 169–177.

- 708 **Ort DR, Merchant SS, Alric J, et al.** 2015. Redesigning photosynthesis to sustainably meet
709 global food and bioenergy demand. *Proceedings of the National Academy of Sciences of the*
710 *United States of America* **112**, 8529–8536.
- 711 **Osorio S, Ruan Y-L, Fernie AR.** 2014. An update on source-to-sink carbon partitioning in
712 tomato. *Frontiers in Plant Science* **5**.
- 713 **Paul MJ, Foyer CH.** 2001. Sink regulation of photosynthesis. *Journal of Experimental*
714 *Botany* **52**, 1383–1400.
- 715 **Paul MJ, Pellny TK.** 2003. Carbon metabolite feedback regulation of leaf photosynthesis
716 and development. *Journal of Experimental Botany* **54**, 539–547.
- 717 **Pérez-Harguindeguy N, Díaz S, Garnier E, et al.** 2013. New handbook for standardised
718 measurement of plant functional traits worldwide. *Australian Journal of Botany* **61**, 167.
- 719 **Piepho HP, Buchse A, Emrich K.** 2003. A Hitchhiker’s Guide to Mixed Models for
720 Randomized Experiments. *Journal of Agronomy and Crop Science* **189**, 310–322.
- 721 **Pokhilko A, Ebenhoh O.** 2015. Mathematical modelling of diurnal regulation of
722 carbohydrate allocation by osmo-related processes in plants. *Journal of The Royal Society*
723 *Interface* **12**, 20141357–20141357.
- 724 **Pomeranz Y, Meloan CE.** 1994. Enzymatic Methods. In: Pomeranz Y, In: Meloan CE, eds.
725 *Food Analysis: Theory and Practice*. Boston, MA: Springer US, 506–531.
- 726 **Pons TL, Flexas J, von Caemmerer S, Evans JR, Genty B, Ribas-Carbo M, Bruognoli E.**
727 2009. Estimating mesophyll conductance to CO₂: methodology, potential errors, and
728 recommendations. *Journal of Experimental Botany* **60**, 2217–2234.
- 729 **Porter J, Xie L, Challinor AJ, Cochrane K, Howden S, Iqbal M, Lobell D, Travasso M.**
730 2014. *Food security and food production systems*.
- 731 **van der Putten PEL, Yin X, Struik PC.** 2018. Calibration matters: On the procedure of
732 using the chlorophyll fluorescence method to estimate mesophyll conductance. *Journal of*
733 *Plant Physiology* **220**, 167–172.
- 734 **Ray DK, Mueller ND, West PC, Foley JA.** 2013. Yield Trends Are Insufficient to Double
735 Global Crop Production by 2050. *PLOS ONE* **8**, e66428.
- 736 **Regmi KC, Zhang S, Gaxiola RA.** 2016. Apoplasmic loading in the rice phloem supported
737 by the presence of sucrose synthase and plasma membrane-localized proton pyrophosphatase.
738 *Annals of Botany* **117**, 257–268.
- 739 **Sage RF, Kubien DS.** 2007. The temperature response of C₃ and C₄ photosynthesis. *Plant,*
740 *Cell & Environment* **30**, 1086–1106.
- 741 **Sage RF, Sharkey TD.** 1987. The Effect of Temperature on the Occurrence of O(2) and

- 742 CO₂ Insensitive Photosynthesis in Field Grown Plants. *Plant Physiology* **84**, 658–664.
- 743 **Sage RF, Sharkey TD, Seemann JR.** 1989. Acclimation of photosynthesis to elevated CO₂
- 744 in five C₃ species. *Plant Physiology* **89**, 590–596.
- 745 **Seneweera SP, Conroy JP, Ishimaru K, Ghannoum O, Okada M, Lieffering M, Kim**
- 746 **HY, Kobayashi K.** 2002. Changes in source-sink relations during development influence
- 747 photosynthetic acclimation of rice to free air CO₂ enrichment (FACE). *Functional plant*
- 748 *biology* **29**, 945–953.
- 749 **Seneweera S, Makino A, Mae T, Basra AS.** 2005. Response of Rice to *p* (CO₂)
- 750 Enrichment: The Relationship Between Photosynthesis and Nitrogen Metabolism. *Journal of*
- 751 *Crop Improvement* **13**, 31–53.
- 752 **Sharkey TD.** 1985. Photosynthesis in intact leaves of C₃ plants: Physics, physiology and rate
- 753 limitations. *The Botanical Review* **51**, 53–105.
- 754 **Sharkey TD.** 2015. Understanding carbon partitioning and its role in determining plant
- 755 growth: Understanding carbon partitioning. *Plant, Cell & Environment* **38**, 1963–1964.
- 756 **Sharkey TD.** 2016. What gas exchange data can tell us about photosynthesis: Gas exchange
- 757 data and photosynthesis. *Plant, Cell & Environment* **39**, 1161–1163.
- 758 **Sharkey TD, Stitt M, Heineke D, Gerhardt R, Raschke K, Heldt HW.** 1986. Limitation of
- 759 Photosynthesis by Carbon Metabolism : II. O₂-Insensitive CO₂ Uptake Results from
- 760 Limitation Of Triose Phosphate Utilization. *Plant Physiology* **81**, 1123–1129.
- 761 **Sharkey TD, Vanderveer PJ.** 1989. Stromal phosphate concentration is low during feedback
- 762 limited photosynthesis. *Plant Physiology* **91**, 679–684.
- 763 **Shimoda S.** 2012. Contribution of leaf nitrogen to photosynthetic gas exchange in contrasting
- 764 rice (*Oryza sativa* L.) cultivars during the grain-filling period. *Photosynthetica* **50**, 387–394.
- 765 **Shimoda S, Maruyama A.** 2014. Rice varietal differences in responses of stomatal gas
- 766 exchange to supplemental nitrogen application. *Photosynthetica* **52**, 397–403.
- 767 **Shimono H, Suzuki K, Aoki K, Hasegawa T, Okada M.** 2010. Effect of panicle removal on
- 768 photosynthetic acclimation under elevated CO₂ in rice. *Photosynthetica* **48**, 530–536.
- 769 **Shinano T, Osawa M, Soejima H, Osaki M.** 2006. Effect of panicle removal on cytokinin
- 770 level in the xylem and nitrogen uptake activity of rice. *Soil Science & Plant Nutrition* **52**,
- 771 331–340.
- 772 **Singsaas EL, Ort DR, Delucia EH.** 2004. Elevated CO₂ effects on mesophyll conductance
- 773 and its consequences for interpreting photosynthetic physiology. *Plant, Cell and Environment*
- 774 **27**, 41–50.
- 775 **Sugden C, Donaghy PG, Halford NG, Hardie DG.** 1999. Two SNF1-Related Protein

- 776 Kinases from Spinach Leaf Phosphorylate and Inactivate 3-Hydroxy-3-Methylglutaryl-
777 Coenzyme A Reductase, Nitrate Reductase, and Sucrose Phosphate Synthase in Vitro. *Plant*
778 *Physiology* **120**, 257–274.
- 779 **Sulpice R, Flis A, Ivakov AA, Apelt F, Krohn N, Encke B, Abel C, Feil R, Lunn JE, Stitt**
780 **M.** 2014. Arabidopsis Coordinates the Diurnal Regulation of Carbon Allocation and Growth
781 across a Wide Range of Photoperiods. *Molecular Plant* **7**, 137–155.
- 782 **Sun Y, Gu L, Dickinson RE, et al.** 2014. Asymmetrical effects of mesophyll conductance on
783 fundamental photosynthetic parameters and their relationships estimated from leaf gas
784 exchange measurements: Asymmetrical mesophyll conductance effects. *Plant, Cell &*
785 *Environment* **37**, 978–994.
- 786 **Tang L, Gao H, Yoshihiro H, Koki H, Tetsuya N, Liu T, Tatsuhiko S, Xu Z.** 2017. Erect
787 panicle super rice varieties enhance yield by harvest index advantages in high nitrogen and
788 density conditions. *Journal of Integrative Agriculture* **16**, 1467–1473.
- 789 **Tazoe Y, von Caemmerer S, Badger MR, Evans JR.** 2009. Light and CO₂ do not affect the
790 mesophyll conductance to CO₂ diffusion in wheat leaves. *Journal of Experimental Botany* **60**,
791 2291–2301.
- 792 **Thompson M, Gamage D, Hirotsu N, Martin A, Seneweera S.** 2017. Effects of Elevated
793 Carbon Dioxide on Photosynthesis and Carbon Partitioning: A Perspective on Root Sugar
794 Sensing and Hormonal Crosstalk. *Frontiers in Physiology* **8**.
- 795 **Urban L.** 2004. Effect of fruit load and girdling on leaf photosynthesis in *Mangifera indica* L.
796 *Journal of Experimental Botany* **55**, 2075–2085.
- 797 **Wang J, Wang C, Chen N, Xiong Z, Wolfe D, Zou J.** 2015. Response of rice production to
798 elevated [CO₂] and its interaction with rising temperature or nitrogen supply: a meta-analysis.
799 *Climatic Change* **130**, 529–543.
- 800 **Wang J, Zhao T, Yang B, Zhang S.** 2018. Sucrose Metabolism and Regulation in
801 Sugarcane. *Journal of Plant Physiology & Pathology* **2017**.
- 802 **Wang M, Zheng Q, Shen Q, Guo S.** 2013. The Critical Role of Potassium in Plant Stress
803 Response. *International Journal of Molecular Sciences* **14**, 7370–7390.
- 804 **Wei H, Meng T, Li X, Dai Q, Zhang H, Yin X.** 2018. Sink-source relationship during rice
805 grain filling is associated with grain nitrogen concentration. *Field Crops Research* **215**, 23–38.
- 806 **Weng J-H, Chen C-Y.** 1991. Effect of Accumulated Nonstructural Carbohydrates on
807 Photosynthesis of Rice Leaves. *Japanese Journal of Crop Science* **60**, 320–321.
- 808 **Weng X-Y, Zheng C-J, Xu H-X, Sun J-Y.** 2007. Characteristics of photosynthesis and
809 functions of the water–water cycle in rice (*Oryza sativa*) leaves in response to potassium

810 deficiency. *Physiologia Plantarum* **131**, 614–621.

811 **White AC, Rogers A, Rees M, Osborne CP.** 2016. How can we make plants grow faster? A
812 source–sink perspective on growth rate. *Journal of Experimental Botany* **67**, 31–45.

813 **Wu A, Song Y, van Oosterom EJ, Hammer GL.** 2016. Connecting Biochemical
814 Photosynthesis Models with Crop Models to Support Crop Improvement. *Frontiers in Plant*
815 *Science* **7**.

816 **Yang F, Liang Z, Wang Z, Chen Y.** 2008. Relationship Between Diurnal Changes of Net
817 Photosynthetic Rate and Influencing Factors in Rice under Saline Sodic Stress. *Rice Science*
818 **15**, 119–124.

819 **Yang JT, Preiser AL, Li Z, Weise SE, Sharkey TD.** 2016. Triose phosphate use limitation
820 of photosynthesis: short-term and long-term effects. *Planta* **243**, 687–698.

821 **Yang J, Zhang J.** 2010. Crop management techniques to enhance harvest index in rice.
822 *Journal of Experimental Botany* **61**, 3177–3189.

823 **Yin X, Sun Z, Struik PC, Gu J.** 2011. Evaluating a new method to estimate the rate of leaf
824 respiration in the light by analysis of combined gas exchange and chlorophyll fluorescence
825 measurements. *Journal of Experimental Botany* **62**, 3489–3499.

826 **Yoshida H, Horie T.** 2009. A process model for explaining genotypic and environmental
827 variation in growth and yield of rice based on measured plant N accumulation. *Field Crops*
828 *Research* **113**, 227–237.

829 **Yoshida H, Horie T, Shiraiwa T.** 2008. A model for explaining genotypic and
830 environmental variation in vegetative biomass growth in rice based on observed LAI and leaf
831 nitrogen content. *Field Crops Research* **108**, 222–230.

832 **Yoshimoto M, Oue H, Kobayashi K.** 2005. Energy balance and water use efficiency of rice
833 canopies under free-air CO₂ enrichment. *Agricultural and Forest Meteorology* **133**, 226–246.

834 **Zhang S, He X, Zhao J, et al.** 2017. Identification and validation of a novel major QTL for
835 harvest index in rice (*Oryza sativa* L.). *Rice (New York, N.Y.)* **10**, 44.

836 **Zhu C, Xu X, Wang D, Zhu J, Liu G, Seneweera S.** 2016. Elevated atmospheric [CO₂]
837 stimulates sugar accumulation and cellulose degradation rates of rice straw. *GCB Bioenergy*
838 **8**, 579–587.

839

840

Table 1: Photosynthesis characteristics (A : for Exp1 and B : for Exp2) measured two weeks after heading on the flag leaf on the main culm of IR64 plants grown under two [CO₂] levels, with panicle pruned at heading (PR) or not (Control). Average values ± standard errors (n=5) are presented. For each column within a [CO₂] level, values followed by different letters differ significantly (P<0.05)

A	[CO ₂] 400 μmol mol ⁻¹	Sampling	Treatment	A (μmol m ⁻² s ⁻¹)	g _s (mmol m ⁻² s ⁻¹)	C _i (μmol mol ⁻¹)	V _{cmax} (μmol m ⁻² s ⁻¹)	J _{max} (μmol m ⁻² s ⁻¹)	TPU (μmol m ⁻² s ⁻¹)	g _m (μmol m ⁻² s ⁻¹ Pa ⁻¹)	SPAD
				Control							
		Morning		23,03 ± 1,18 a	598,15 ± 21,21 a	321,82 ± 9,67 a	93,80 ± 8,66 a	142,80 ± 10,98 a	10,74 ± 0,60 a	12,65 ± 0,57 a	45,66 ± 0,76 a
		Midday		21,84 ± 0,96 a	572,50 ± 28,37 a	309,75 ± 2,35 ab	96,50 ± 3,13 a	136,00 ± 3,55 a	10,05 ± 0,26 ab	13,10 ± 0,62 a	45,01 ± 0,74 a
		Afternoon		21,48 ± 1,54 a	525,32 ± 59,35 a	316,57 ± 6,15 ab	89,60 ± 7,78 a	126,20 ± 6,75 a	9,70 ± 0,37 ab	11,93 ± 0,95 a	44,40 ± 0,54 a
			PR								
		Morning		22,68 ± 0,74 a	541,06 ± 45,72 a	311,16 ± 6,33 ab	90,20 ± 4,55 a	132,00 ± 6,24 a	9,32 ± 0,36 ab	12,48 ± 0,16 a	47,00 ± 1,87 a
		Midday		19,38 ± 1,89 a	393,47 ± 91,60 ab	286,36 ± 15,43 ab	88,40 ± 4,85 a	123,20 ± 1,98 a	8,76 ± 0,49 ab	12,58 ± 0,72 a	46,86 ± 1,17 a
		Afternoon		18,38 ± 1,00 a	281,24 ± 33,01 b	277,85 ± 8,39 b	90,60 ± 6,13 a	125,80 ± 7,23 a	8,38 ± 0,57 b	12,38 ± 0,56 a	47,28 ± 0,92 a
	[CO ₂] 800 μmol mol ⁻¹	Sampling	Treatment	A (μmol m ⁻² s ⁻¹)	g _s (mmol m ⁻² s ⁻¹)	C _i (μmol mol ⁻¹)	V _{cmax} (μmol m ⁻² s ⁻¹)	J _{max} (μmol m ⁻² s ⁻¹)	TPU (μmol m ⁻² s ⁻¹)	g _m (μmol m ⁻² s ⁻¹ Pa ⁻¹)	SPAD
			Control								
		Morning		24,28 ± 0,47 a	709,38 ± 27,47 a	326,58 ± 4,73 a	95,50 ± 3,51 a	144,75 ± 5,92 a	10,85 ± 0,41 a	13,21 ± 0,73 a	45,25 ± 0,80 a
		Midday		22,48 ± 0,1,09 a	662,15 ± 33,46 ab	327,55 ± 3,01 a	88,80 ± 4,24 a	134,60 ± 8,35 a	10,10 ± 0,58 a	13,01 ± 0,64 a	46,14 ± 0,27 a
		Afternoon		21,76 ± 1,41 a	576,29 ± 84,55 ab	317,58 ± 13,10 ab	94,00 ± 5,54 a	134,40 ± 5,01 a	9,94 ± 0,27 a	12,20 ± 1,06 a	47,04 ± 1,06 a
			PR								
		Morning		21,36 ± 1,29 a	576,28 ± 85,35 ab	312,40 ± 8,89 ab	85,50 ± 3,97 ab	136,25 ± 2,86 a	9,33 ± 0,20 ab	12,44 ± 0,66 a	46,16 ± 0,65 a
		Midday		19,98 ± 1,22 a	431,54 ± 55,71 b	301,39 ± 6,68 ab	85,20 ± 1,59 ab	128,40 ± 4,83 a	9,16 ± 0,35 ab	12,21 ± 0,53 a	47,05 ± 0,75 a
		Afternoon		10,94 ± 0,92 b	168,36 ± 9,15 c	282,15 ± 7,11 b	64,80 ± 9,51 b	116,40 ± 10,06 a	7,88 ± 0,39 b	12,50 ± 0,44 a	44,58 ± 1,70 a
B	[CO ₂] 400 μmol mol ⁻¹	Sampling	Treatment	A (μmol m ⁻² s ⁻¹)	g _s (mmol m ⁻² s ⁻¹)	C _i (μmol mol ⁻¹)	V _{cmax} (μmol m ⁻² s ⁻¹)	J _{max} (μmol m ⁻² s ⁻¹)	TPU (μmol m ⁻² s ⁻¹)	g _m (μmol m ⁻² s ⁻¹ Pa ⁻¹)	SPAD
			Control								
		Midday		21,44 ± 0,94 a	465,18 ± 38,50 a	291,70 ± 6,82 a	97,40 ± 3,50 a	144,60 ± 2,97 a	10,08 ± 0,30 a	12,12 ± 0,78 a	44,98 ± 1,24 a
		Afternoon		20,73 ± 0,46 ab	427,13 ± 37,20 ab	280,29 ± 6,75 ab	91,60 ± 7,59 a	141,20 ± 4,98 a	9,96 ± 0,16 a	12,93 ± 0,51 a	44,30 ± 1,53 a
		Evening		20,49 ± 0,52 ab	375,91 ± 5,72 ab	278,72 ± 9,05 bc	95,2 ± 2,95 a	131,00 ± 5,21 a	9,54 ± 0,21 ab	11,97 ± 0,89 a	44,06 ± 0,67 a
			PR								
		Midday		20,70 ± 0,56 ab	395,71 ± 36,66 ab	277,95 ± 5,77 ab	100,40 ± 5,31 a	133,60 ± 4,50 a	9,14 ± 0,27 abc	11,87 ± 0,85 a	45,48 ± 0,85 a
		Afternoon		19,32 ± 0,52 ab	296,42 ± 32,02 bc	251,56 ± 5,49 bc	96,80 ± 1,98 a	130,80 ± 4,21 a	8,74 ± 0,24 bc	11,30 ± 0,65 a	44,30 ± 1,49 a
		Evening		18,06 ± 0,55 b	261,15 ± 11,78 c	228,23 ± 12,32 c	87,00 ± 4,91 a	127,20 ± 3,72 a	8,30 ± 0,17 c	11,15 ± 0,72 a	45,09 ± 0,98 a
	[CO ₂] 800 μmol mol ⁻¹	Sampling	Treatment	A (μmol m ⁻² s ⁻¹)	g _s (mmol m ⁻² s ⁻¹)	C _i (μmol mol ⁻¹)	V _{cmax} (μmol m ⁻² s ⁻¹)	J _{max} (μmol m ⁻² s ⁻¹)	TPU (μmol m ⁻² s ⁻¹)	g _m (μmol m ⁻² s ⁻¹ Pa ⁻¹)	SPAD
			Control								
		Midday		22,89 ± 0,51 a	560,16 ± 32,49 a	302,28 ± 6,24 a	93,80 ± 3,56 a	138,60 ± 5,79 a	10,38 ± 0,21 a	13,80 ± 0,59 a	47,80 ± 0,68 a
		Afternoon		22,26 ± 0,60 a	420,84 ± 39,11 b	289,06 ± 10,12 ab	91,80 ± 8,34 a	135,80 ± 5,97 a	10,06 ± 0,29 a	10,02 ± 0,50 c	46,76 ± 1,28 a
		Evening		21,35 ± 0,64 a	360,9 ± 10,46 bc	287,98 ± 13,67 ab	91,00 ± 2,56 a	129,60 ± 7,65 ab	9,70 ± 0,29 a	12,15 ± 0,51 abc	46,02 ± 0,56 a
			PR								
		Midday		20,63 ± 0,45 a	409,25 ± 13,58 b	279,86 ± 5,06 ab	88,60 ± 4,30 ab	128,80 ± 3,30 ab	9,42 ± 0,33 a	12,98 ± 0,72 ab	47,94 ± 1,69 a
		Afternoon		13,21 ± 0,37 b	275,55 ± 6,62 c	258,18 ± 2,12 b	67,60 ± 3,66 b	120,20 ± 4,27 ab	7,78 ± 0,07 b	10,62 ± 0,75 bc	47,50 ± 0,98 a
		Evening		10,85 ± 0,65 b	147,47 ± 6,35 d	256,23 ± 4,05 b	65,50 ± 5,47 b	107,00 ± 8,22 b	6,38 ± 0,35 c	10,10 ± 0,49 c	47,08 ± 0,73 a

Table 2: Nonstructural carbohydrate contents, raw data (A : for Exp1 and B : for Exp2) measured two weeks after heading in the flag leaf, the upper and lower internode on the main culm of IR64 plants grown under two air CO₂ levels, with panicle pruned at heading (PR) or not (Control). Average values ± standard errors (n=5) are presented. For each column within a [CO₂] level, values followed by different letters differ significantly (P<0.05).

A

[CO ₂] 400 μmol mol ⁻¹	Sampling	Treatment	Sucrose flag leaf (μg cm ⁻²)	Sucrose lower internode (mg g ⁻¹ DM)	Hexose flag leaf (μg cm ⁻²)	Hexose lower internode (mg g ⁻¹ DM)	Starch flag leaf (μg cm ⁻²)	Starch upper internode (mg g ⁻¹ DM)	Starch lower internode (mg g ⁻¹ DM)
Control									
	Morning		191,17 ± 23,57 b	150,67 ± 37,61 a	16,02 ± 4,95 a	11,65 ± 4,40 a	83,07 ± 35,01 a	134,76 ± 44,89 b	245,23 ± 60,21 b
	Midday		234,21 ± 45,89 ab	205,92 ± 15,09 a	28,76 ± 6,61 a	5,27 ± 0,79 ab	125,66 ± 19,73 a	187,78 ± 23,86 ab	275,73 ± 67,09 ab
	Afternoon		270,82 ± 24,87 ab	190,22 ± 38,72 a	25,75 ± 3,81 a	5,36 ± 1,01 ab	82,85 ± 12,73 a	163,16 ± 14,42 ab	233,97 ± 70,05 b
PR									
	Morning		231,81 ± 36,16 b	103,53 ± 23,33 a	20,48 ± 6,40 a	2,19 ± 0,50 b	84,39 ± 31,10 a	311,88 ± 30,32 a	519,13 ± 22,72 a
	Midday		286,91 ± 28,58 ab	116,68 ± 7,17 a	26,50 ± 5,43 a	2,27 ± 0,29 b	53,02 ± 11,54 a	311,50 ± 38,84 a	424,59 ± 16,60 ab
	Afternoon		395,74 ± 34,50 a	116,83 ± 35,88 a	26,32 ± 4,18 a	2,93 ± 0,53 b	127,95 ± 35,12 a	323,19 ± 46,70 a	531,41 ± 44,68 a
[CO ₂] 800 μmol mol ⁻¹	Sampling	Treatment	Sucrose flag leaf (μg cm ⁻²)	Sucrose lower internode (mg g ⁻¹ DM)	Hexose flag leaf (μg cm ⁻²)	Hexose lower internode (mg g ⁻¹ DM)	Starch flag leaf (μg cm ⁻²)	Starch upper internode (mg g ⁻¹ DM)	Starch lower internode (mg g ⁻¹ DM)
Control									
	Morning		211,07 ± 17,99 d	162,40 ± 26,30 a	20,14 ± 4,95 a	5,39 ± 1,25 a	118,68 ± 57,70 a	466,75 ± 26,74 a	402,95 ± 87,42 a
	Midday		275,96 ± 20,25 cd	134,89 ± 32,73 a	35,35 ± 9,28 a	5,87 ± 2,80 a	140,17 ± 27,54 a	402,87 ± 83,40 a	361,65 ± 83,60 a
	Afternoon		374,44 ± 17,42 ab	109,29 ± 31,38 a	28,02 ± 2,32 a	3,73 ± 0,96 a	299,80 ± 69,52 a	403,31 ± 38,06 a	466,65 ± 55,21 a
PR									
	Morning		289,59 ± 35,19 bcd	77,14 ± 36,31 a	28,59 ± 2,77 a	1,86 ± 0,77 a	231,67 ± 78,24 a	476,33 ± 71,84 a	580,20 ± 59,77 a
	Midday		361,39 ± 13,51 bc	81,31 ± 25,90 a	37,80 ± 5,49 a	1,82 ± 0,45 a	309,85 ± 85,62 a	357,17 ± 37,35 a	530,03 ± 40,33 a
	Afternoon		466,86 ± 24,82 a	80,86 ± 9,98 a	38,27 ± 1,63 a	2,17 ± 0,28 a	249,24 ± 69,02 a	511,71 ± 56,08 a	641,20 ± 26,05 a

B

[CO ₂] 400 μmol mol ⁻¹	Sampling	Treatment	Sucrose flag leaf (μg cm ⁻²)	Sucrose lower internode (mg g ⁻¹ DM)	Hexose flag leaf (μg cm ⁻²)	Hexose lower internode (mg g ⁻¹ DM)	Starch flag leaf (μg cm ⁻²)	Starch upper internode (mg g ⁻¹ DM)	Starch lower internode (mg g ⁻¹ DM)
Control									
	Midday		310,98 ± 55,11 b	161,37 ± 10,79 a	22,34 ± 5,64 a	12,99 ± 3,85 ab	44,20 ± 8,28 a	170,36 ± 47,47 ab	156,27 ± 41,56 a
	Afternoon		355,45 ± 28,85 b	180,03 ± 14,49 a	18,05 ± 1,10 a	14,71 ± 2,35 a	70,08 ± 10,64 a	93,63 ± 15,00 b	178,80 ± 35,69 a
	Evening		430,43 ± 59,40 ab	132,44 ± 12,12 a	21,55 ± 3,91 a	13,32 ± 0,83 b	117,66 ± 31,14 a	157,34 ± 55,66 ab	147,55 ± 65,72 a
PR									
	Midday		311,76 ± 33,78 b	139,35 ± 13,67 a	17,17 ± 1,13 a	8,97 ± 2,03 ab	48,51 ± 8,99 a	170,59 ± 32,28 ab	362,25 ± 51,80 a
	Afternoon		490,53 ± 23,50 ab	141,84 ± 9,84 a	26,10 ± 1,42 a	8,00 ± 2,08 ab	94,55 ± 8,97 a	202,02 ± 19,43 ab	288,21 ± 68,60 a
	Evening		496,92 ± 37,84 a	134,44 ± 20,75 a	28,81 ± 3,65 a	5,72 ± 1,57 ab	128,38 ± 33,51 a	299,98 ± 53,68 a	294,26 ± 63,43 a
[CO ₂] 800 μmol mol ⁻¹	Sampling	Treatment	Sucrose flag leaf (μg cm ⁻²)	Sucrose lower internode (mg g ⁻¹ DM)	Hexose flag leaf (μg cm ⁻²)	Hexose lower internode (mg g ⁻¹ DM)	Starch flag leaf (μg cm ⁻²)	Starch upper internode (mg g ⁻¹ DM)	Starch lower internode (mg g ⁻¹ DM)
Control									
	Midday		267,33 ± 27,60 b	105,41 ± 3,38 a	20,17 ± 2,72 a	8,53 ± 4,35 a	53,16 ± 15,27 a	110,36 ± 16,20 b	184,22 ± 55,74 a
	Afternoon		352,10 ± 40,06 ab	93,10 ± 3,78 a	26,24 ± 4,07 a	9,40 ± 2,24 a	104,30 ± 17,14 a	54,03 ± 7,15 b	168,88 ± 60,77 a
	Evening		393,25 ± 18,79 a	106,22 ± 8,73 a	20 ± 2,31 a	3,72 ± 1,07 a	149,94 ± 23,65 a	80,99 ± 16,68 b	164,39 ± 52,57 a
PR									
	Midday		382,65 ± 16,76 ab	97,01 ± 17,13 a	24,47 ± 3,23 a	4,23 ± 0,83 a	50,82 ± 11,22 a	282,52 ± 32,88 a	352,03 ± 49,52 a
	Afternoon		423,82 ± 33,98 a	85,91 ± 9,68 a	24,15 ± 4,96 a	2,35 ± 0,16 a	104,30 ± 32,82 a	240,88 ± 31,66 a	338,46 ± 37,24 a
	Evening		452,95 ± 12,27 a	96,18 ± 5,58 a	23,70 ± 3,51 a	3,84 ± 0,62 a	131,61 ± 39,77 a	267,47 ± 30,55 a	323,30 ± 37,70 a

Figure legends

Fig. 1: Effect of pruning and CO₂ treatment on photosynthetic parameters, (A) net assimilation rate A , (B) triose phosphate utilization TPU, (C) maximum carboxylation rate of Rubisco V_{cmax} , and (D) maximum rate of electron transport J_{max} . Measured at 2 weeks after heading on the flag leaf on the main culm of plants of IR64 rice genotype at two CO₂ levels (400 and 800 $\mu\text{mol mol}^{-1}$), in two growth chambers for experiments 1 and 2. Black symbol: Control (plants with panicles) and red symbol: PR (plants with panicle pruned). Measurements were carried out at morning (mor), midday (mid), afternoon (aft) and evening (eve) periods. Stars indicate significant difference at $p < 0.05$ (Tukey HSD test) among values. NS: not significant. Each point represents the mean of 5 values \pm SE.

Fig. 2: Mean A/C_i curves for all treatment combination (A) and corresponding mean $\phi\text{PSII}/C_i$ curves (B) for experiments 1 and 2 (shown only for Pruning treatment which caused significant TPU decline). Dashed lines indicate mean C_i value (290 $\mu\text{mol mol}^{-1}$) for photosynthesis measurement at treatment CO₂ level (400 or 800 $\mu\text{mol mol}^{-1}$). Arrows in Fig. 2B indicates the C_i level at which TPU limitation may begin to occur. The CO₂ concentrations indicated in Figure headers are treatment conditions and not those administered when measuring CO₂ response, which comprised 14 different levels.

Fig. 3: Relationship between TPU and net photosynthesis (A) within experiments 1 and 2 and for each combination of CO₂ x panicle pruning treatment. With panicle and 400 $\mu\text{mol mol}^{-1}$ (black symbol), with panicle and 800 $\mu\text{mol mol}^{-1}$ (grey symbol), Panicles pruned and 400 $\mu\text{mol mol}^{-1}$ (red symbol), panicles pruned and 800 $\mu\text{mol mol}^{-1}$ (yellow symbol). Each point represents a single value.

Fig. 4: Relationship between TPU and Leaf sucrose content in experiments 1 and 2, separating control and panicle pruning treatment. With panicle at 400 $\mu\text{mol mol}^{-1}$ (black symbol), with panicle at 800 $\mu\text{mol mol}^{-1}$ (grey symbol), Panicles pruned at 400 $\mu\text{mol mol}^{-1}$ (red symbol), panicles pruned at 800 $\mu\text{mol mol}^{-1}$ (yellow symbol). Dashed lines represent linear regression for both pruning treatments. Each point is the average of 5 values and is presented with horizontal and vertical standard errors.

Fig. 5: Relationship between TPU and local source-sink ratio (defined as flag leaf area / spikelet number on the main culm) in experiments 2. Line represents linear regression.

Fig. 1:

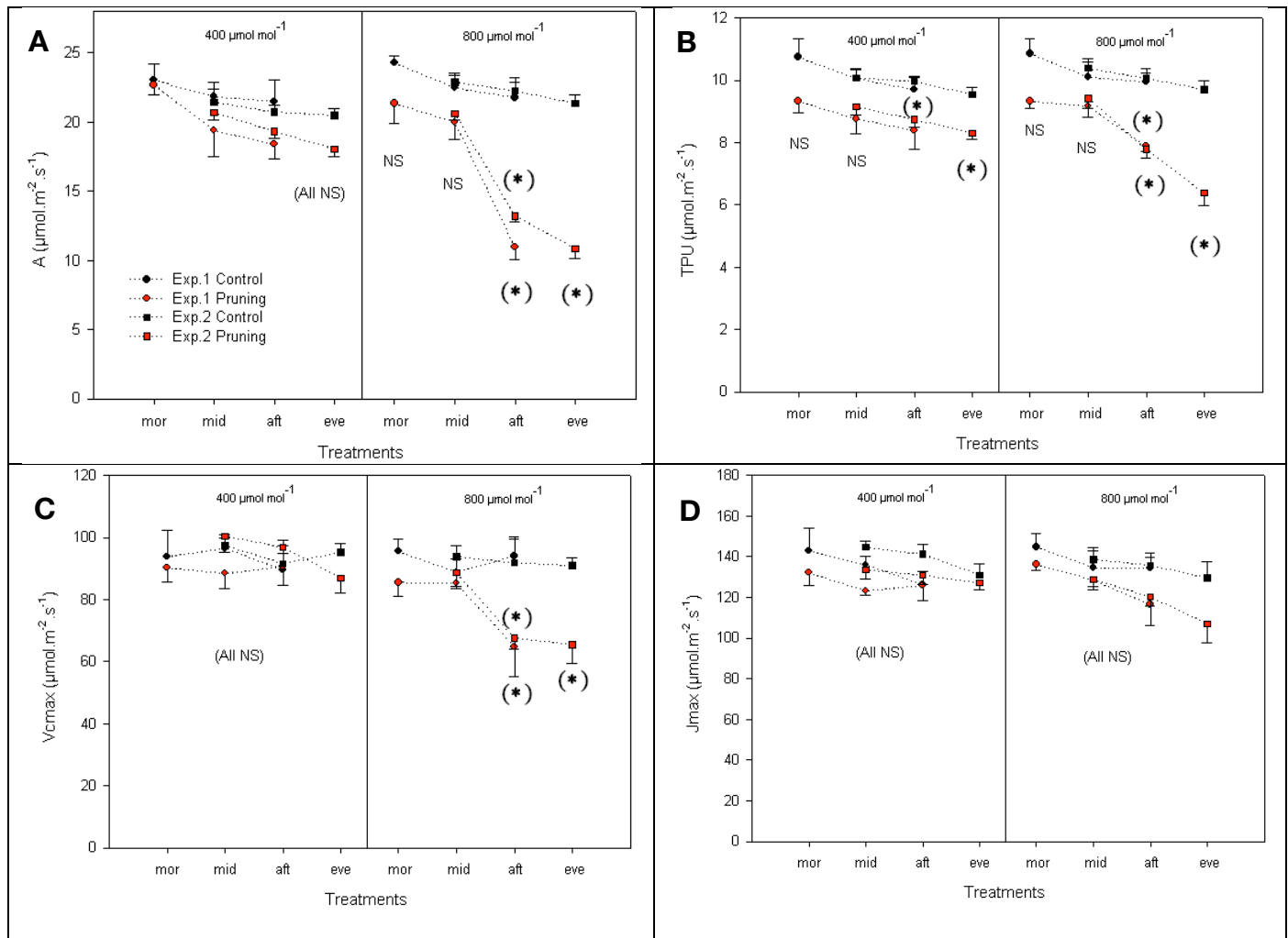


Fig. 2:

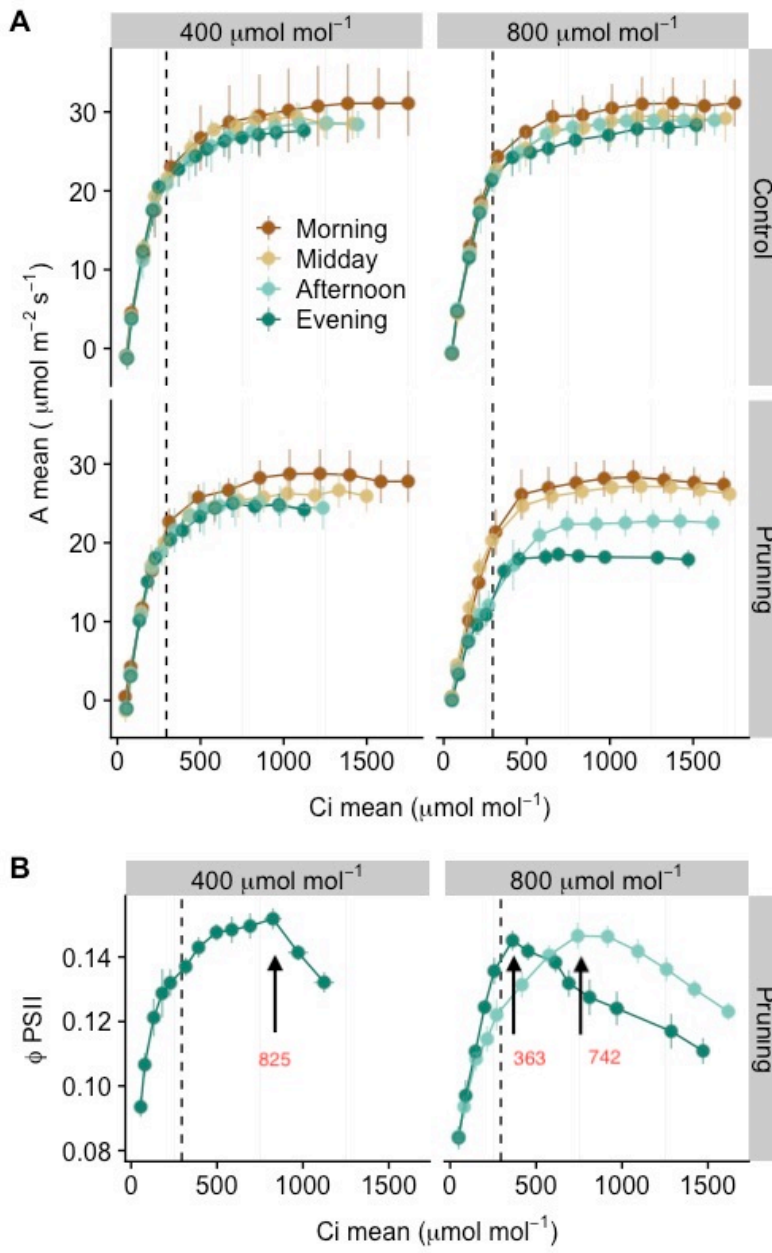


Fig. 3:

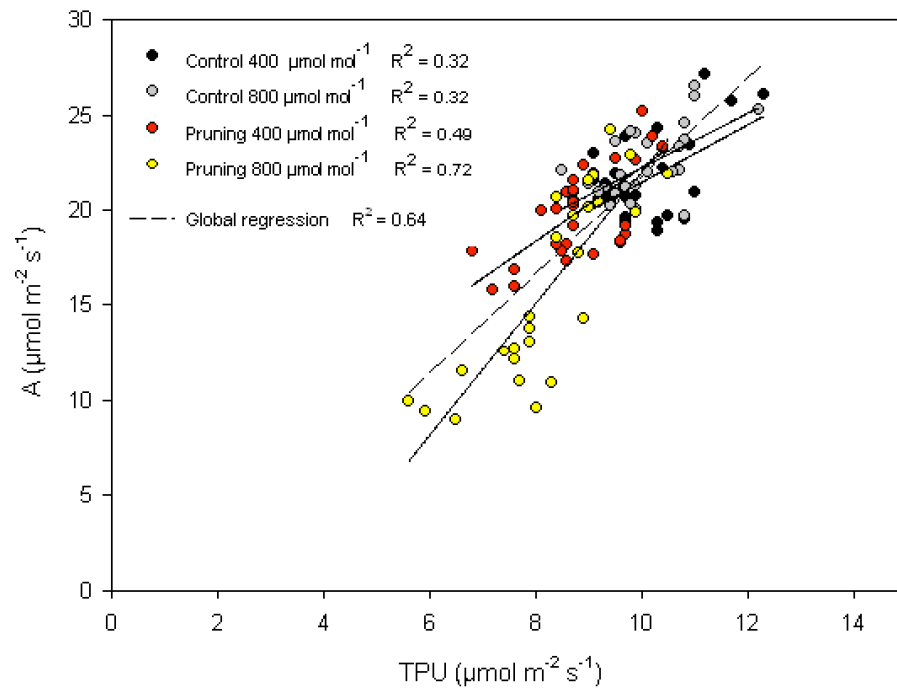


Fig. 4:

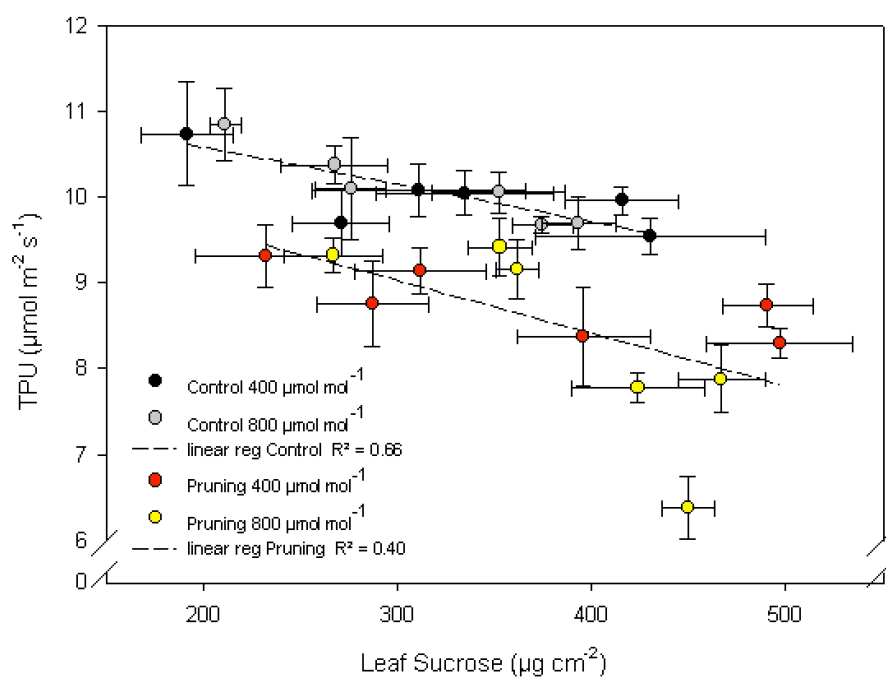


Fig. 5:

